NTNU
Norwegian University of
Science and Technology

Effect of Anisotropy, Strain Rate and Progressive Failure in Numerical Simulations of the Shear Vane Test

Kristian Rismyhr

Civil and Environmental Engineering
Submission date: June 2017
Supervisor: Steinar Nordal, IBM
Co-supervisor: Jon Ronningen, IBM

Norwegian University of Science and Technology
Department of Civil and Environmental Engineering

NORWEGIAN UNIVERISTY OF SCIENCE AND TECHNOLOGY-
DEPARTMENT OF CIVIL AND ENVIRONMENTAL ENGINEERING

Report Title:	**Date: 09.06.2017**	
Effect of Anisotropy, Strain Rate, and Progressive Failure in Numerical Simulations of the Shear Vane Test	**Number of pages:** 106	
	Master Thesis	x
Name: Kristian Rismyhr		
Professor in charge/supervisor: Steinar Nordal (NTNU)		
Other supervisors: Jon A. Rønningen (NTNU)		

Abstract:
The shear vane test is a method of determining the in-situ undrained strength and remolded shear strength of cohesive soils. During the shear vane test, an increasing torque is applied until the surrounding soil goes to failure. When the torque at failure is known, the shear strength can be determined by means of an idealized and simplified formula which correlates torque and shear strength.

Previous tests have shown that that several aspects of cohesive soil material behavior such as anisotropy, strain softening (progressive failure) and strain rate, which are not incorporated in the idealized and simplified formula, affect the measured strength from the shear vane test. This implies that the interpretation of the undrained shear strength from the shear vane test is more complicated than the simplified and idealized formula used today.

In this report, numerical simulations have been conducted in Plaxis 2D and Plaxis 3D in order to investigate to which extent progressive failure (softening), anisotropy and strain rate affect the measured strength from the shear vane test. The material models used were Mohr-Coulomb, Geofuture Soft Clay (a user defined material model developed by NTNU) and the total stress based NGI ADP model.

The Mohr Coulomb material model was applied in Plaxis 2D and 3D to determine the effects of progressive failure. From the Mohr-Coulomb simulations conducted, the effect of progressive failure from the 2D and 3D simulations were 2 % and 4% respectively. The simulations conducted seem to suggest that the effect of progressive failure can be neglected when using the Mohr-Coulomb material model.

The Geofuture material model was applied in Plaxis 2D to determine the effects of strain rate during the shear vane test. Several simulations were conducted in which the time to failure varied. Based on the simulations conducted, a tenfold increase in time to failure decreases the measured strength by 7-8%.

The NGI ADP material model was applied in Plaxis 3D to determine to which extent anisotropy affects the strength determined in the shear vane test. The degree of anisotropy was measured by the plasticity index (I_p). For each simulation the active shear strength was kept constant while the direct and passive strengths varied as a function of I_p. Based on the simulations conducted, the torque at failure increases by 4 % per 10 % increase in I_p.

Keywords:

1. Shear vane test
2. Anisotropy
3. Progressive failure (softening)
4. Strain rate

Kristian Rismyhr

NTNU – Trondheim
Norwegian University of
Science and Technology

MSc Thesis

TBA4900 – Geotechnical Engineering

Spring 2017
By
Kristian Rismyhr

Title: Effect of Anisotropy, Strain Rate, and Progressive Failure in Numerical Simulations of the Shear Vane Test

BACKGROUND

The undrained shear strength is essential for design of geotechnical structures involving clay. There are several methods to determine undrained strength, both in the field and in the laboratory. Today, cone penetration testing with porepressure measurements is the dominating method. Some years ago the in-situ shear vane test was very popular, but the vane test is rarely used in today's geotechnical field investigations. This is mainly due to uncertainties in interpretation of the test results, even though the basic principles of the test apparently are simple. So called correction factors have been suggested for the interpretation, but why they are needed is not fully understood.

PROBLEM FORMULATION

For low plastic clays the undrained shear strength is anisotropic showing different strengths under active, direct and passive conditions. The vane gives a strength that is neither of these three. Further, the undrained shear strength is rate dependent. While an undrained laboratory test may take hours, the vane test may take seconds. Strain softening after reaching a peak strength is another complicating factor. It has been suggested that if a sensitive or quick clay is tested, a progressive failure mechanism occurs around the vane and that the interpreted strength is much lower than the peak strength.

This MSc work aims to study some of these effects through a finite element analysis (FEA) with appropriate soil models in PLAXIS. A vane test is to be simulated in two- and three-dimensional models. Comparing the resulting, simulated force with an expected force based directly on input peak strength(s) the effect of softening, anisotropy and rate of loading is to be studied.

Professor in charge:

Steinar Nordal (NTNU)

Co-supervisor:

Jon A. Rønningen (NTNU)

Department of Civil and Environmental Engineering, NTNU

Professor in Charge

Preface

The following report is a master thesis in geotechnics as part of the MSc in Civil and Environmental Engineering at NTNU. The thesis was carried out during the spring semester of 2017. This report corresponds to a total work load of 30 ECTS points equivalent to one semester of study.

Trondheim, 2017-06-09

Kristian Rismyhr

Acknowledgment

Firstly, I would like to send my respect and gratitude to the division of Geotechnical Engineering at NTNU whom has offered excellent supervision and contributed to a pleasant study environment during the writing of this thesis.

A special thanks goes to Steinar Nordal for his advice, support and constructive criticism during the writing of this report.

I would also like to thank Dr.Gylland for his advice and suggestions to the literature survey.

Last, but not least, I am deeply thankful for the support received by PhD candidate Jon Rønningen who has put his knowledge and valuable time to my disposal.

K.R.

(K.R)

Abstract

The shear vane test is a method of determining the in-situ undrained strength and remolded shear strength of cohesive soils. During the shear vane test, an increasing torque is applied until the surrounding soil goes to failure. When the torque at failure is known, the shear strength can be determined by means of an idealized and simplified formula which correlates torque and shear strength.

Previous tests have shown that several aspects of cohesive soil material behavior such as anisotropy, strain softening (progressive failure) and strain rate, which are not incorporated in the simplified formula, affect the measured strength from the shear vane test. This implies that the interpretation of the undrained shear strength from the shear vane test is more complicated than the simplified and idealized formula used today.

In this report, numerical simulations have been conducted in Plaxis 2D and Plaxis 3D in order to investigate to which extent progressive failure (softening), anisotropy and strain rate affect the measured strength from the shear vane test. The material models used were Mohr-Coulomb, Geofuture Soft Clay (a user defined material model developed by NTNU) and the total stress based NGI ADP model.

The Mohr-Coulomb material model was applied in Plaxis 2D and 3D to determine the effects of progressive failure. From the Mohr-Coulomb simulations conducted, the effect of progressive failure from the 2D and 3D simulations were 2 % and 4% respectively. The simulations conducted seem to suggest that the effect of progressive failure can be neglected when using the Mohr-Coulomb material model.

The Geofuture material model was applied in Plaxis 2D to determine the effects of strain rate during the shear vane test. Several simulations were conducted in which the time to failure varied. Based on the simulations conducted, a tenfold increase in time to failure decreases the measured strength by 7-8%.

The NGI ADP material model was applied in Plaxis 3D to determine to which extent anisotropy affects the strength determined in the shear vane test. The degree of anisotropy was measured by the plasticity index (I_p) of the soil. For each simulation the active shear strength was kept constant while the direct and passive strengths varied as a function of I_p. Based on the simulations conducted, the torque at failure increases by 4 % per 10 % increase in I_p.

Sammendrag

Vingeboret er et in-situ instrument for bestemmelse av uforstyrret udrenert skjærstyrke og omrørt skjærstyrke til kohesjonsjordarter. Under forsøket blir vingen påført et økende moment helt til jorda rundt går til brudd. Udrenert skjærfasthet kan tolkes fra det maksimale målte momentet ved hjelp av en idealisert og forenklet formel.

Tidligere forsøk har vist at flere aspekter av materialoppførsel til kohesjonsjordarter som anisotropi, softening (progressiv bruddutvikling) og tøyningshastighet påvirker den målte skjærstyrken fra vingeborforsøket. Disse aspektene er ikke tatt hensyn til i den forenklede formelen. Dette impliserer at tolkning av vingeborforsøket er mer komplisert enn den forenklede formelen som brukes i dag.

I denne rapporten har numeriske simuleringer blitt gjennomført i Plaxis 2D and Plaxis 3D for å undersøke til hvilken grad progressiv bruddutvikling (softening), anisotropi og tøyninghastighet påvirker den målte skjærstyrken fra vingeborforsøket. Materialmodellene som har blitt brukt er Mohr-Coulomb, Geofuture Soft Clay (en brukerdefinert materialmodell utviklet av NTNU) og den totalspenningsbaserte materialmodellen NGI ADP.

Mohr Coulomb ble brukt i Plaxis 2D og Plaxis 3D for å finne ut til hvilken grad progressiv bruddutvikling (softening) påvirker det målte momentet i vingeborforsøket. Fra Mohr-Coulomb simuleringene i Plaxis 2D og Plaxis 3D ble effektene av progressiv bruddutvikling fastslått til henholdsvis 2% og 4%. Dermed indikerer simuleringen at effekten av progressivbrudd påvirker den målte momentet i neglisjerbar grad når Mohr-Coulomb materialmodellen er brukt.

Geofuture materialmodellen ble brukt i Plaxis 2D for å undersøke effektene av tøyningshastighet under vingeborforsøket. Flere simuleringer ble gjennomført, hvor tid til brudd varierte for hver simulering. Basert på simuleringene gjort, kan det tyde på at en ti dobling av tid til brudd, reduserer det målte momentet med 7-8 %.

NGI ADP modellen ble brukt i Plaxis 3D for å undersøke til hvilken grad anisotropi påvirker det målte momentet under vingeborforsøket. Korrelasjonsparameteren plastisitetsindeks, I_p, ble brukt for å angi grad av anisotropi. Den aktive skjærstyrken var konstant for hver simulering, mens den passive og direkte skjærstyrken varierte som en funksjon av I_p. Fra simuleringene gjort, kan det tyde på at det målte momentet reduseres med 4% per 10% økning i I_p.

Contents

List of Figures

List of Tables

Chapter 1

Introduction

The undrained shear strength is essential for design of geotechnical structures involving clay. There are several methods to determine undrained strength, both in the field and in the laboratory. One of the methods is the shear vane test. The shear vane test is a cheap and easily executed test. Since the shear vane test is cheap and easily executed one would think that it is commonly used in Norway, but this is not the case.

There are several reasons for the lack of vane test usage, and these will be discussed further in this report. In the last years, there has been interest from NTNU and Norwegian Public Roads Administration to examine the vane test's potential in Norway. The shear vane test could have great potential as a quick clay detector as it the only test that can determine the sensitivity of a soil in-situ.

1.1 Background

Some years ago the in-situ shear vane test was very popular, but the vane test is rarely used in today's geotechnical field investigations. This is partly due to the increasing use of CPTU but uncertainties in the interpretation and lack of reliability of the shear vane test results is also a factor.

When determining the shear strength from the shear vane test a simplified and idealized formula which correlates the torque at failure and shear strength is used. This formula is based on several assumptions regarding material behavior of cohesive soils. These assumptions include isotropic soil, non progressive failure and a cylindrical uniform and fully mobilized shear surface at failure.

Previous shear vane tests have shown that the resistance and the failure mechanism of the

soil during the shear vane test is, contrary to the assumptions in the simplified formula, influenced by factors such as inherent soil anisotropy, strain rate and strain softening. This implies that the interpretation of the undrained shear strength is more complicated than the simplified and idealized formula used today.

So called correction factors have been been suggested for the intrepretation of the test results, but why there are needed is not fully understood.

1.2 Scope

The work proposed for this MSc research is to create a better platform for understanding and interpreting shear vane test results. This MSc work aims to study the effects of anisotropy, progressive failure (softening) and strain rate through a finite element analysis (FEA) with appropiate soil models in Plaxis. The vane is simulated in two- and three- dimensional models.

The aim of this MSC research is achieved by:

1. Conducting a literature survey of the shear vane test, cohesive soil material behavior, factors influencing the shear vane test results and the different correction factors.
2. Conducting numerical analysis of the shear vane test.

Literature Survey

There has been a lot of research regarding the shear vane test. The literature survey part of this report focuses on Scandinavian research. In Norway Bjerrum (1972), Aas (1965),and Karlsrud et al. (2005) have been most prominent in this field. Additionally NTNU (2014) and NIFS have collaborated the last years, to check the shear vane test's potential and limitations as a quick clay detector. Swedish Geotechnical Institute and their state of the art Information 3 handbook (Larsson et al. (2007)) is also discussed.

Numerical Analysis

The numerical analysis in this report will be done in the finite element method program Plaxis. Several material models will be used, in order to examine the different aspects of cohesive soil material behavior.

1.3 Outline of Thesis

The report consists of two main parts:

1. Part I : Theoretical Background
2. Part II : Numerical Analysis

Part I (Theoretical Background) consists of the following chapters:

- Chapter 2 - Shear vane test
  - This chapter gives a introduction of the shear vane test, including the apparatus, procedure and interpretation of results.
- Chapter 3 - Factors influencing the shear vane tests results
  - This chapter contains a literature study of the factors influencing the results from the shear vane test, including cohesive soil material behavior.
- Chapter 4 - Correction Factor
  -This chapter contains a literature study of the correction factors proposed in Scandinavia.

Part II (Numerical Analysis) consists of the following chapters:

- Chapter 5 - Material Models
  -This chapter gives a brief introduction to the material models used in the simulations.
- Chapter 6 - Model and Material Parameters
  -This chapter summarizes the values for each material parameter. In addition, the Plaxis models and mesh used in the simulations are shown.
- Chapter 7 - Results and Discussions
  - This chapter presents and discusses the results from the numerical simulations.
- Chapter 8 - Conclusion
  - This chapter summarizes the work done and offers a recommendation for further work.

Part I

Theoretical Background

Chapter 2

Shear Vane Test

The shear vane test is a method for determining the undrained shear strength, remolded shear strength and sensitivity of cohesive soils.

Early geotechnical engineers had difficulties determining the shear strength of very soft and sensitive clays by means of laboratory tests due to high disturbance induced by poor quality samplers. These difficulties led to the development of the shear vane test. The shear vane test, an in-situ test, isn't affected by sample disturbance to the same extent as laboratory tests. The vane device made it possible, for the first time, to determine the undrained shear strength and remolded shear strength in-situ. Since the shear vane test is the only method of determining the sensitivity of a clay in-situ, it can be used as an effective quick clay detector.

2.1 Apparatus

As shown in the figure 2.1, the apparatus consists of a 4 bladed rectangular vane connected to a system of inner rods. Conventionally, the height to diameter ratio of each blade is two. In Norway either blades of diameter 65 or 55 mm are used. The largest vane (65mm) is convenient to use in soft and sensitive clays with an undrained shear strength less than 50 kPa. The smaller vane (55mm) is commonly used in clays with an undrained shear strength between 30 and 100 kPa. The conventional thickness of each blade is 2 mm. Generally, the shear vane test is only conducted in cohesive soils (primarily clay).

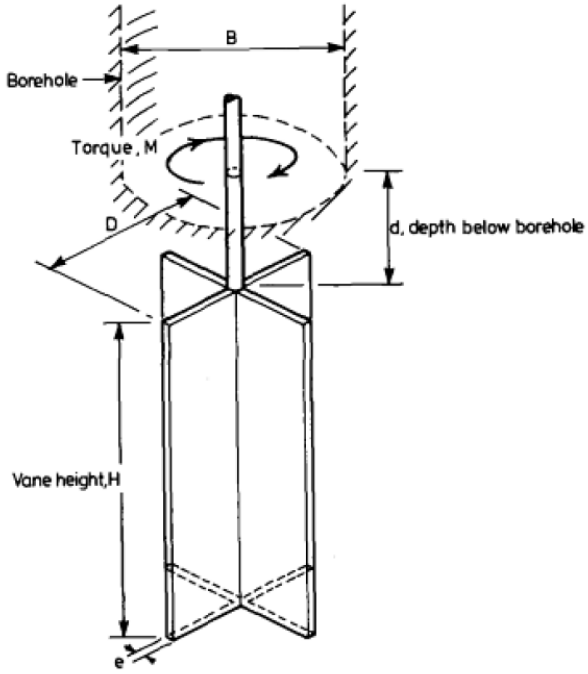

Figure 2.1: Field vane test apparatus (after (Chandler, 1988))

2.2 Procedure

During penetration to the required depth, the vane is withdrawn and protected in a shoe vane connected to the outer roads. When the desired depth is reached, a torque measuring device is mounted on top of the inner rods as shown in Figure 2.1. An increasing torque is applied until the soil around the vane goes to failure.

The remolded shear strength is determined after 25 rotations, subsequent to the initial failure. To eliminate or reduce the possible effect of friction another reading is recorded when the blade is turned 90 degrees. The lowest remolded shear strength is chosen.

During the test it is important to avoid any rotation of the vane, and check that the friction in the rods is negligible . The shear vane test should be done within 5 minutes after insertion of the vane to avoid re-consolidation of the soil. A maximum rate of rotation of 12 degrees per minute is recommended and the area ratio should be less than 12%. A change in rotation speed will affect the measured undrained shear strength. The shorter the 'time to failure' is, the higher the measured undrained shear strength will be. In Norway it is required that the time to failure is between one and three minutes. A constant time to failure eliminates most of the problems concerning the twisting of the rods, which can for some test be several times larger than the actual rotation of the blade.

2.3 Interpretation

When the torque at failure is known from the shear vane test, one can determine the average uncorrected peak shear strength and the remoulded shear strength using the general formula below.

$$s_u = \frac{\kappa}{\kappa + 1} \cdot \frac{T_{total}}{\pi D^3} \tag{2.1}$$

where

s_u is the undrained shear strength from the vane test

D is the diameter of vane

T_{total} is the measured torque

and κ is a constant describing the shear stress distribution around the top and bottom of the vane.

The formula is based on the the total applied torque (consisting of a horizontal component and a vertical component) being equal to the integrals of the shear stresses acting between the adjacent soil and the vane. Conventionally it is assumed that the undrained shear strength is fully mobilized along a circular shear surface as shown in Figure 2.2 below. The failure surface shown in Figure 2.2 yields a κ value of 6.

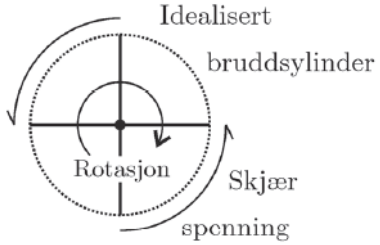

Figure 2.2: Assumed geometry of the failure surface (after (NTNU, 2014))

If the failure geometry in Figure 2.2 is assumed, then the total torque in the horizontal plane (T_h) is:

$$T_h = 2\int_0^{\frac{D}{2}} 2\pi r^2 \tau \, dr$$

$$T_h = \frac{\pi D^3 s_{uh}}{6} \tag{2.2}$$

where s_{uh} is the undrained shear strength in the horizontal plane.

Likewise the torque in the vertical plane (T_v) is:

$$T_v = \pi D H \tau \cdot \frac{D}{2} = \frac{\pi D^2 H s_{uv}}{2}$$

$$T_v = \pi D^3 s_{uv} \tag{2.3}$$

where s_{uv} is the undrained shear strength in the vertical plane.
The total torque is the sum of the torques in the horizontal and vertical planes. Adding the two equations above, and solving it with respect to the undrained shear vane shear strength (s_u) gives the following undrained shear strength formula:

$$s_u = \frac{6T_{total}}{7\pi D^3} \tag{2.4}$$

The formula above is assuming an isotropic soil, implying that the undrained shear strength in the horizontal plane (s_{uh}) is equal to the undrained shear strength in the vertical plane (s_{uv}). This is commonly done in shear vane test interpretation, and this assumption will be discussed in further detail later in this report. A more thorough explanation and derivation of the measured torque during the shear vane test is done in section 7.1.

As previously mentioned, κ in the general formula (equation 2.1) depends on the assumed shear stress distribution. A circular failure which is assumed above yields a κ value of 6. A triangular shear distribution would result in a κ value of 8.

2.4 Assumptions

Formula 2.4 is based on several assumptions that include:

- Homogeneous soil
- Isotropic soil
- Insertion of the vane causes no or negligible disturbance
- No drainage occurs during the test,i.e. no consolidation takes place when inserting the vane or during the test
- Cylindrical, uniform and fully mobilized shear surface at failure
- Non progressive failure

Chapter 3

Factors Influencing The Shear Vane Tests Results

Studies from Norwegian Geotechnical Institute (NGI) and Swedish Geotechnical Institute (SGI) showed that the shear vane test did not yield the same undrained shear strength as laboratory tests. The laboratory tests were done on block samples of high quality. NGI and SGI argued that the strength determined the shear vane test (using the simplified equation 2.4) was not representative for the clays tested.

Back calculations done by NGI have shown that some slopes that have yet to fail have a factor of safety less than 1 when using the simplified formula (equation 2.4). Likewise there have been done back calculations of known failure slopes where the factor of safety was determined to be greater than 1.

Depending on the situation, the undrained strength determined from the shear vane test, were either conservative or non conservative. Regardless of the degree of conservatism, these back calculations show how unreliable the measured undrained shear strength determined by the shear vane test can be. Unreliable results is a major reason why vane test usage has declined in Norway in the last decades.

There are several factors why a discrepancy between the measured undrained shear strength from the shear vane test and the undrained shear strength from laboratory tests exists. It is mainly due to the fact that the assumptions mentioned in section 2.4 are rarely, if ever, going to be correct. Material behavior, that isn't taken into consideration in equation 2.4 such as strain rate also plays a role.

In this chapter several factors which affect the shear vane test results will be discussed.

3.1 Non Homogeneous Soil

Contrary to the first assumption in section 2.4, no soil is completely homogeneous. The shear vane test is sensitive to heterogenities. A thin layer of silt or sand would cause local drainage (one assumes undrained behaviour when conducting the vane test). Any contact between the vane and a non-clay material would affect the measured s_u. If drainage causes the soil to consolidate, the measured strength would increase. The non homogeneous nature of soils will always be a factor when conducting the shear vane test.

3.2 Waiting Time

The waiting period (the time between inserting the vane and rotating the vane by an applied torque) will affect the measured s_u. A longer waiting period causes the soil to consolidate, thus increasing the measured s_u. This effect can be observed in figure 3.1 below:

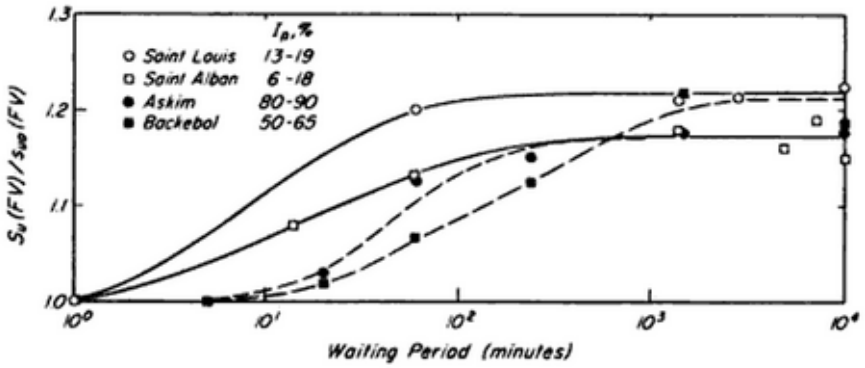

Figure 3.1: Correlation between waiting time and measured s_u (after (Terzaghi et al., 1996))

To avoid diverging test data, the vane test has a standard waiting time of 3-5 minutes.
In general, waiting time does not influence the measured s_u from the vane test to a great extent if the waiting time is within the boundaries of standard waiting time.

3.3 Blade thickness

Blade thickness will also have an effect on the measured s_u. Research from Terzaghi et al. (1996) showed that an increase in blade thickness, decreases the measured s_u.

Terzaghi et al. (1996) findings is summarized in figure 3.2 :

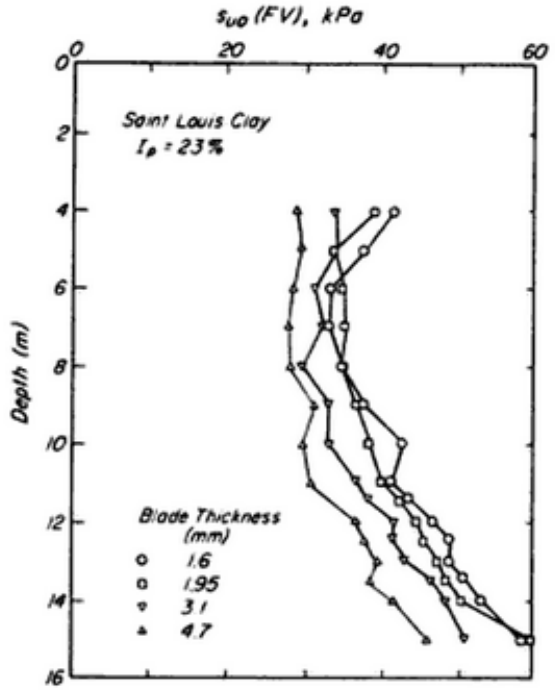

Figure 3.2: Correlation between blade thickness and measured s_u at various depths (after (Terzaghi et al., 1996))

To avoid diverging test data, a standard blade thickness of 2mm is commonly used in Norway.

In general, blade thickness does not influence the measured s_u from the vane test to a great extent if blades with standard blade thickness of 2mm are used.

3.4 Soil Anisotropy

Contrary to the second assumption in section 2.4 ; no cohesive soil is isotropic.

Soil anisotropy is a main reason why the measured undrained shear strength from the vane test differs from those determined by laboratory tests. The simplified formula (Formula 2.4) does not incorporate soil anisotropy. When performing the shear vane one can not be certain if it simulates an active,direct or passive test (or something in between). The active, direct and passive strengths determined in the laboratory will be different ; due to soil anisotropy. In the simplified formula (Formula 2.4) one assumes an isotropic soil, implying that the undrained shear strength on the vertical surface is equal to the undrained shear strength on the horizontal surface.

There exists two kinds of soil anisotropy ; inherent anisotropy and stress induced anisotropy. Inherent stress anisotropy refers to the soil structure orientation at micro-level. Stress inducted anisotropy is caused by different horizontal and vertical stresses. In practice, it is difficult to distinguish these two kinds of anisotropy. Conventionally one refers to the combined effect of both kinds in geotechnical practice.

Due to anisotropy of cohesive soils, the undrained shear strength will vary with loading direction. As shown in the figure 3.3 below, there will be several shear zones in a shear surface; direct shear zone, active shear zone and passive shear zone. These zones will differ in stress directions and will, due to soil anisotropy, exhibit a different shear strength.

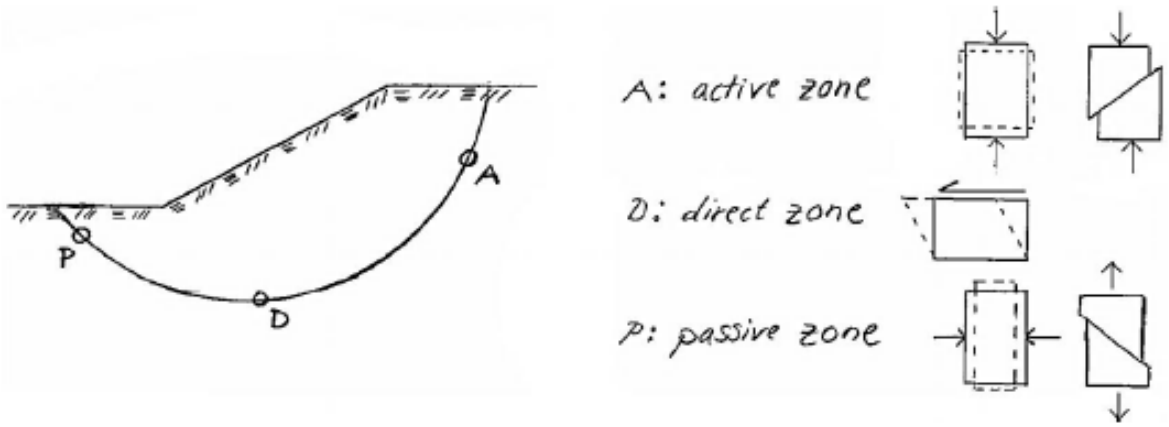

Figure 3.3: Shear zones in a slope stability problem (after (Larsson et al., 2007))

Laboratory tests from Jamiolkowski et al. (1985) which is summarized in figure 3.4 below show how the undrained shear strength varies with the direction of shear.

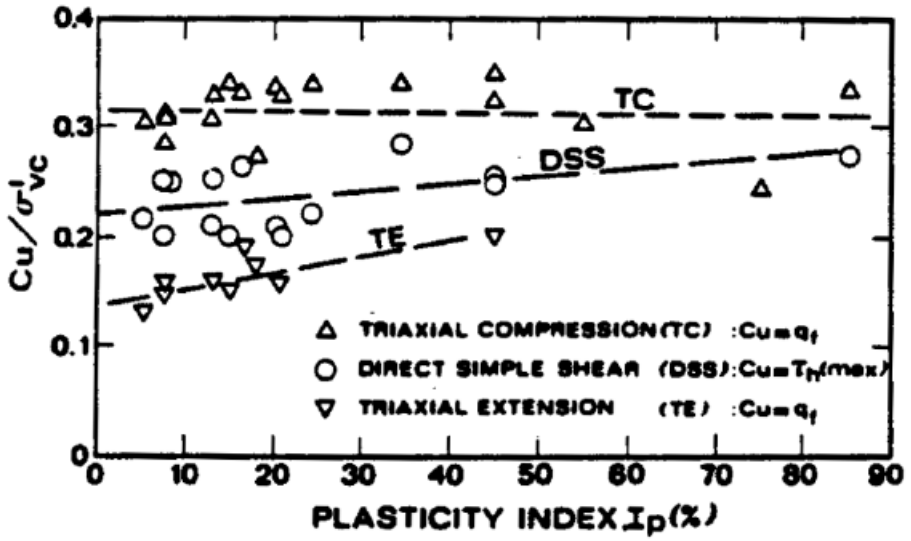

Figure 3.4: Undrained shear strength normalized with vertical stress with varying plasticity (after (Jamiolkowski et al., 1985))

In the figure above, tri-axial compression (active), direct simple shear (direct) and tri-axial extension (passive) tests (normalized with respect to the vertical stress) are plotted with respect to plasticity index.

In the diagram one can observe that all three tests (passive,direct and active) yield different undrained shear strengths. The undrained shear strength will vary with its loading direction. Additionally, one can observe that the differences in the three undrained shear strengths decreases as the plasticity index increases.

The findings regarding the correlation between degree of soil anisotropy and plasticity index from Jamiolkowski et al. (1985) in Figure 3.4 is confirmed by Fauskerud et al. (2013).

Fauskerud et al. (2013) discovered the following relation :

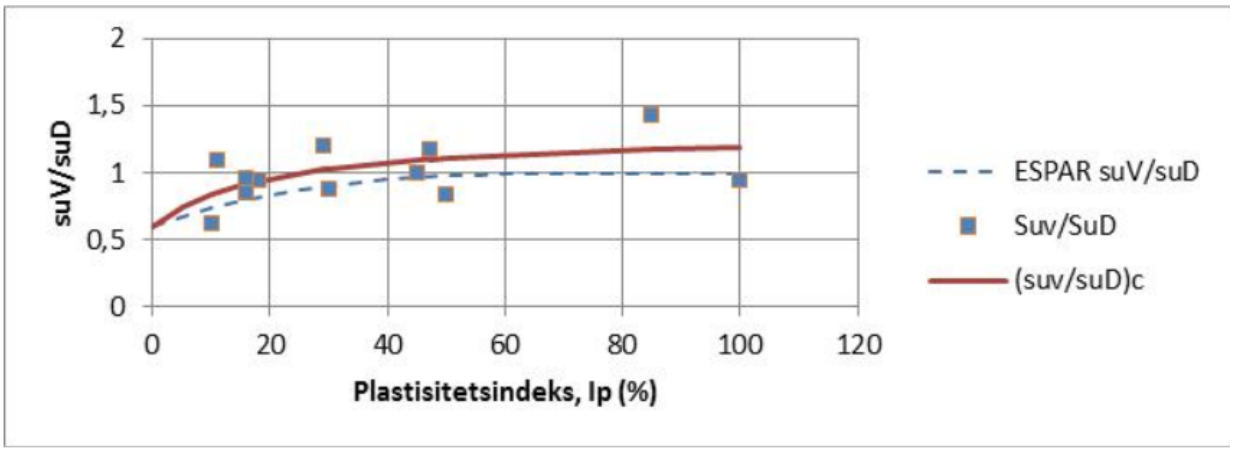

Figure 3.5: Anisotropy correlations for NC, non-sensitive clays (after (Fauskerud et al., 2013))

Figure 3.5 shows the correlation between the degree of anisotropy of a clay and its plasticity index. The greater the plasticity index is, the more isotropic the soil is. Brittle Norwegian clays, which have low plasticity, will therefore be very anisotropic. This is of great importance when determining the shear strength of quick clay using the vane test.

3.4.1 General Empirical Relation

Ladd and Foott (1974) created a general empirical relation in order to estimate the shear strength of a soil. This empirical relation is known as the SHANSEP (Stress History And Normalized Soil Engineering Properties) method. The method is based on the observation that the shear strength of many soils can be normalized with respect to the vertical consolidation pressure. Using the SHANSEP method the undrained shear strength of a soil can be determined using the following relation:

$$\tau_{fu} = S \cdot \sigma'_{v0} \cdot (OCR)^m \tag{3.1}$$

where

τ_{fu} is the undrained strength of the soil

S is a material parameter

m is a material parameter

σ'_{V0} is the vertical effective stress

OCR is the over consolidation ratio

3.4.2 Norwegian Empirical Relation

Basing his study on the SHANSEP method, (Karlsrud et al., 2005) presented results of shear strength results taken with a block sampler. Anisotropic consolidated undrained compression tests were conducted. Using the SHANSEP relation he determined values of constants S and m in the active shear zone that are representative for Norwegian clays. His findings are summarized in Figure 3.6 below.

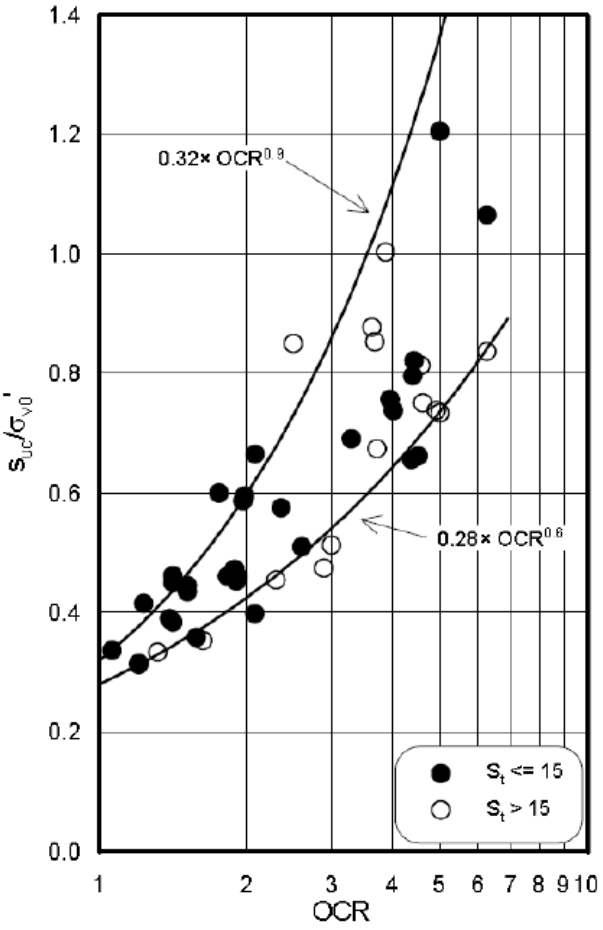

Figure 3.6: Normalized strength values for block samples in relation to OCR (after (Karlsrud et al., 2005))

From the figure one can observe that the upper and lower bounds of the active undrained shear strength are respectively approximated to

$$\tau_{fu}^{A} \approx 0.32 \cdot \sigma_0^{'} \cdot OCR^{0.9} \tag{3.2}$$

$$\tau_{fu}^{A} \approx 0.28 \cdot \sigma_0^{'} \cdot OCR^{0.6} \tag{3.3}$$

Often the active undrained shear strength is simplified to the average of the upper and lower bound:

$$s_{u,active} = 0.3 \cdot \sigma_v^{'} \tag{3.4}$$

In the same manner; direct and passive undrained shear strength are often simplified to

$$s_{u,direct} = 0.2 \cdot \sigma_v^{'} \tag{3.5}$$

$$s_{u,passive} = 0.1 \cdot \sigma_v^{'} \tag{3.6}$$

respectively.

The three simplified undrained shear strength relations (equations 3.4, 3.5 and 3.6) underlines that cohesive soils are indeed anisotropic. The undrained shear strength of the soil will depend on the loading direction. The inherent anisotropic behavior of cohesive soils is the biggest flaw in the assumptions mentioned in 2.4. As a consequence of the anisotropic nature of cohesive soils, the measured undrained shear strength from the shear vane test is usually "corrected" with respect to the degree of anisotropy (anisotropy is often measured by the plasticity index) of the soil.

3.5 Strain Softening and Progressive Failure

As mentioned in section 2.4, conventionally one assumes a fully mobilized cylindrical shear failure around the vane, implying no progressive failure. This is not the case for quick clay. Norwegian brittle and low plastic clays, with high content of silt, are especially susceptible to progressive failure as they exhibit a strain softening behavior.

As previously discussed, there is an active, direct and passive zone in a slope stability problem. Each zone will exhibit a different strength due to soil anisotropy.

In figure 3.7 from Ladd (1991) one can observe a shear stress strain plot of the active, direct and passive zone for a slope stability failure of a contractant clay.:

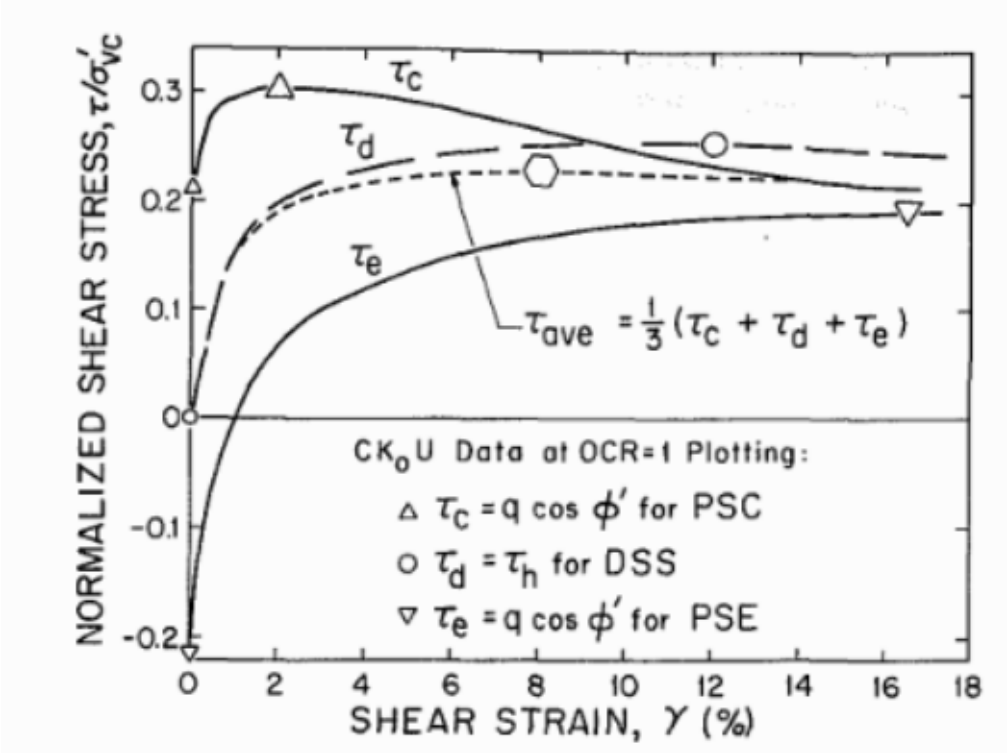

Figure 3.7: Normalized stress strain data for a cay illustrating progressive failure and strain softening (after (Ladd, 1991))

τ_c, τ_d,τ_e represent the resistance of the active (compression), direct and passive(extension) portion respectively.

As one can observe from the figure 3.7, the resistance in the compression zone against shear decreases after reaching its peak strength (softening) at about 2 % strain. Meanwhile the resistance in the extension and direct zones requires large strains to reach their maximum strengths. These data show that the compression zone will be strained beyond its peak strength and lose resistance before the direct and extension zones are fully mobilized. This is what the phenomenon of progressive failure implies. In a progressive failure the total resistance mobilized along the active, direct and passive failure surface will be smaller the sum of their individual peak strengths. A clay with post peak softening will progressively fail. Progressive failure also implies non uniform stress and strain conditions.

Gylland (2012) states that: "The mechanism behind strain softening behaviour is not related to change in material parameters, but rather a consequence of the open structure. When sheared under undrained conditions there is no possibility of volume change and the contractancy induces excess pore pressures. In turn the effective stress, and thus the shear strength, is reduced as the stress state is forced to move down along the Mohr-Coulomb line."

The figures below show a progressively developing failure mode of a sensitive clay. Sensitive soft clays, like the one in the figures below, experience a softening behaviour after peak undrained shear strength. As a consequence of the softening behavior, the failure mode will be more "square-rounded" instead of a cylindrical fully mobilized shear failure.

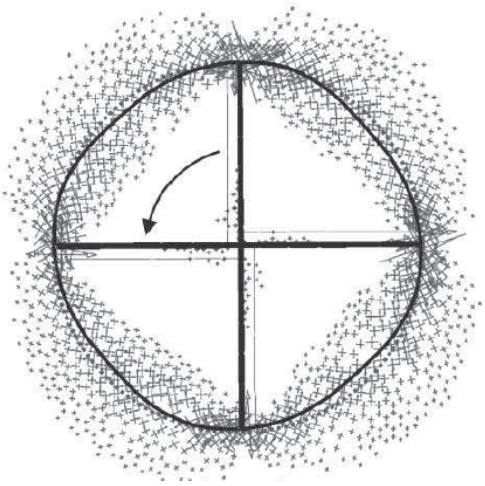

(a) Principal strain directions before global peak (after (Gylland et al., 2012))

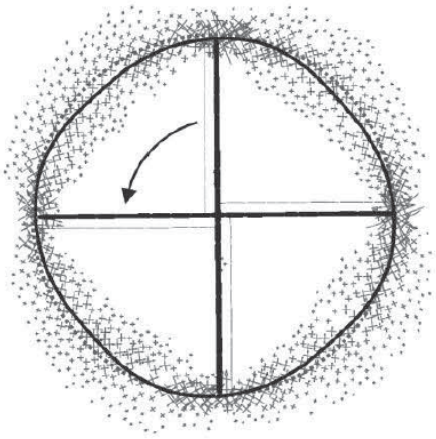

(b) Principal strain directions at global peak (after (Gylland et al., 2012))

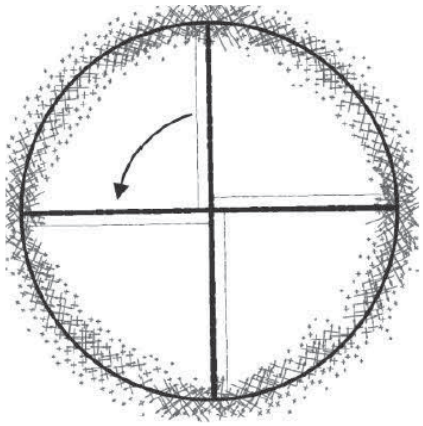

(c) Principal strain directions at residual (after (Gylland et al., 2012))

Figure 3.8: Principal strain directions (After (Gylland et al., 2012))

Gylland (2012) offers an explanation for the square-rounded shape: "For the soil not sheared by the vane blades the failure surface is not restrained to the forced circular kinematics of the problem. In this state the governing stress promotes a rounded square shape. The square shape is also the path of least resistance for the global response. The total solution is then the rounded quadratic shape where the kinematics restrains of the circular failure mode is dominating close to the tip of the blades and the Rankine stress fields are governing the center region."

Cadling and Odenstad (1948) also noticed the progressive failure behavior of clays in Sweden but concluded that the effect of progressive failure was minimal and could be ignored.

Keep in mind,clays in Sweden are generally more plastic and less brittle than clays in Norway. If the shear vane test is to be used as a quick clay detector, one should be aware of that the effect of progressive failure could be significant.

3.6 Strain Rate Effect

Another factor influencing the shear vane test results is the strain rate. Research has shown that the measured peak undrained shear strength depends on the rate of shear. The faster the material goes to failure,the higher the measured shear strength will be. Figure 3.9 and figure 3.10 below from Andersen and Lunne (2007) show this effect:

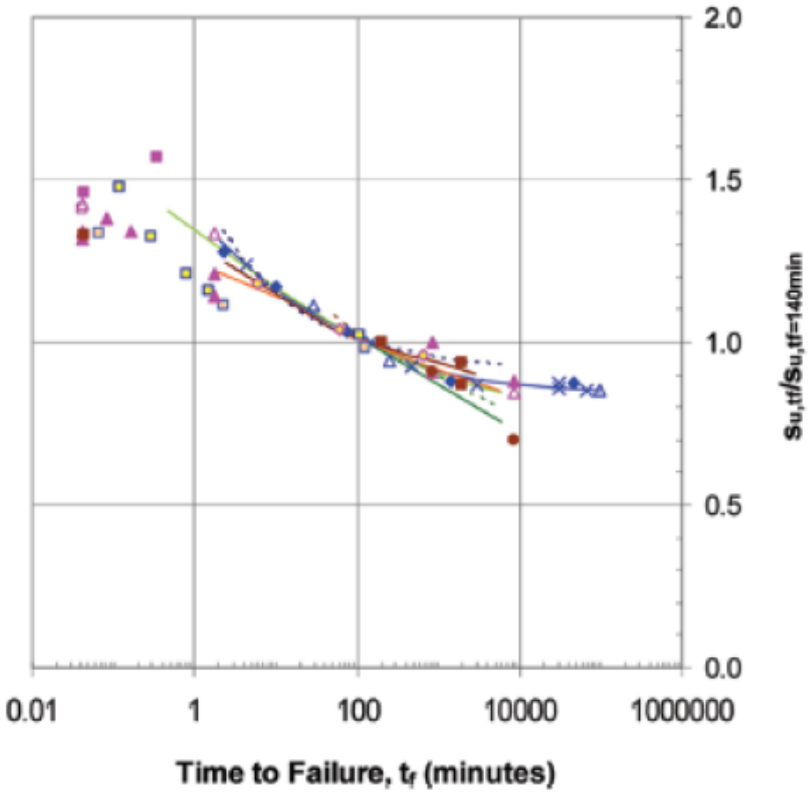

Figure 3.9: Time to failure effects on marine clay (after (Andersen and Lunne, 2007))

The measured undrained shear strength is inversely proportional to the time to failure.

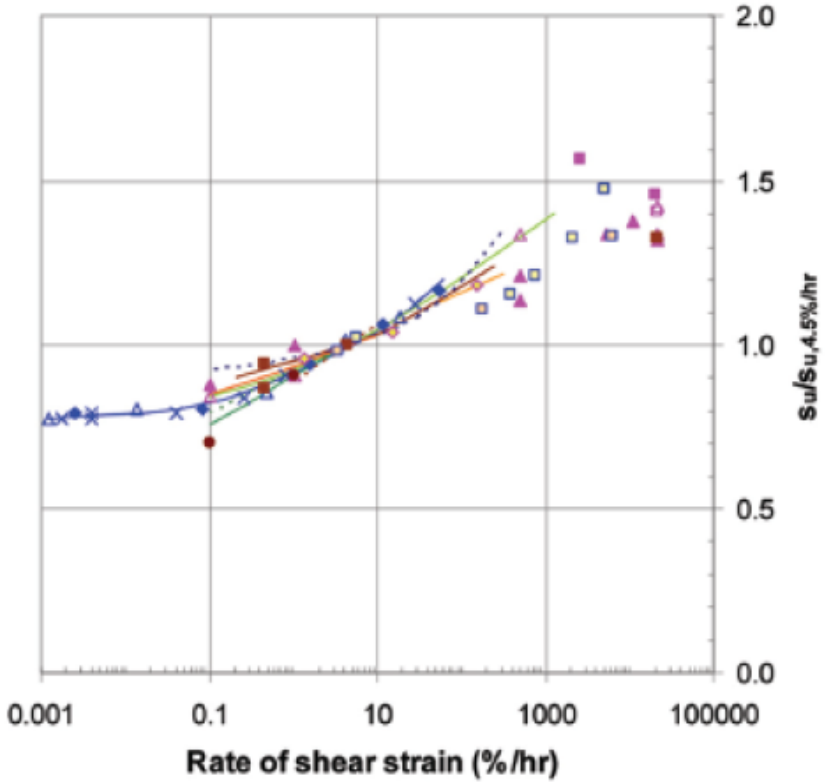

Figure 3.10: Rate of shear strains effects on marine clay (after (Andersen and Lunne, 2007))

The measured undrained shear strength is proportional to the rate of shear.

Dependency of strain rate of soils consists of two components; the viscous effect of the soil and time dependent dissipation of excess pore pressure.

When executing a shear vane test the soil will fail after approximately two minutes (high speed). A standard laboratory test will usually go to failure in the 1-4 hour range (medium speed), yielding lower strength results than the vane test due to a lower strain rate. In a stability problem the time to failure be will be in the magnitude of days or weeks (low speed).

Due to the different strain rates (alternatively different time to failure) in the shear vane test and laboratory tests, one should expect a difference in the measured peak undrained shear strength from the shear vane test and the one determined from laboratory tests.

It is universally agreed that the rate of shear is proportional to the measured peak undrained shear strength. However there are still discussions regarding to which extent an increase in shear rate affects the measured shear strength. Einav and Randolph (2005) argued that the strength increases by between 5% and 20% per order of magnitude increase of the shear rate.

Meanwhile Graham et al. (1983) argued that an increase of 10% to 20% per order of magnitude increase of the shear rate.

The influence of the rate of shear with respect to the residual strength is still discussed. Shear vane tests by Biscotin and Pestana (2001) showed an increase in shear rate yielded a greater peak undrained shear strength but did not influence the residual strength. Contrary to Biscotin and Pestana (2001) findings, Graham et al. (1983) concluded that the strain rate influenced the residual strength. According to Graham et al. (1983) a higher residual is expected for low rates compared to high rates.

Aas et al. (1986) purposed that OCR was a better indicator than plasticity index for determining the factor of strain rate.This was confirmed by Sheahan et al. (1996). The more porous (alternatively the less over consolidated) the clay is, the greater role strain rate plays.

3.7 Conclusion

The factors discussed in this chapter affect the measured undrained shear strength. These factors are not incorporated in the simplified formula (equation 2.4).

Due to these factors there exists a discrepancy between the measured undrained shear strength from the vane test and the one determined from laboratory tests. The most influential factor is soil anisotropy. As discussed, the measured shear strength depends on the orientation of the slip surface. Soil anisotropy is correlated with plasticity index. The greater the plasticity index is, the more isotropic the soil is.

In addition, the vane test and laboratory tests have different strain rates, thus yielding different undrained shear strengths. Other factors such as sample disturbance, heterogeneous soil, local drainage, waiting time, blade thickness and progressive failure also affect the measured undrained shear strength.

Chapter 4

Correction factor

4.1 Vane Correction Factor

Due to discrepancies between the measured undrained shear strength from the vane test and the undrained shear strength determined from laboratory tests, several correction factors have been introduced to correlate these two strengths. Conventionally this correction factor is called μ.

The laboratory tests, which the shear vane test results have been compared with, include isotropic/anisotropic consolidated tri-axial compression/extension, direct shear and simple shear. Not only is the undrained shear strength from the shear vane test different from the undrained shear strength from the laboratory tests, the vane test frequently measures a non-conservative shear strength that would be critical in stability calculations.

Over the years several correction factors have been established. The reason for the discrepancy between the laboratory results and the shear vane results is that the assumptions mentioned in section 2.4 regarding the shear vane test are only to a certain extent true. In the following chapter only the correction factors introduced in Norway and Sweden will be discussed.

The Norwegian and Swedish correction factors are based on Norwegian and Swedish clays respectively. Even though Norwegian and Swedish clays are comparable, they have some different properties. For example, Norwegian clays generally contain more silt, thus making them more brittle and more exposed to progressive failure. This should be taken into account when comparing the different correction factors.

4.2 Swedish Correction Factor

4.2.1 Original Correction Factor

In 1969 the Swedish Geotechnical Institute (SGI) introduced a correction factor to adjust the measured undrained shear strength from the shear vane test. The correction factor (Figure 4.1 below) was based on liquid limit, which is directly correlated to soil anisotropy. The greater the liquid limit is, the more isotropic the soil is.

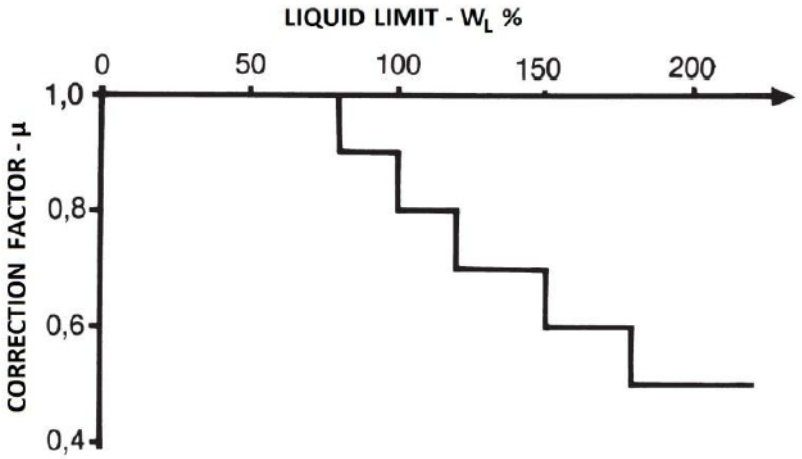

Figure 4.1: SGI correction factor 1969 (after (Larsson et al., 2007))

As this correction factor only was a rough estimate, SGI recommended to use a conservative estimate of the shear strength, to avoid overestimating the strength of the soil.

In the 70s, Swedish geotechnical engineer Helenelund proposed a new correction factor, were Bjerrum's theories regarding plasticity index were converted to liquid limit. Helenelund's theories fitted well with the original Swedish correction factor from 1969 for low liquid limits. There was a greater discrepancy at higher liquid limits but due to overall similar values, SGI decided not to implement Helenelund's correction factor. However, Helenelund's theory formed the basis for SGI's new correction factor in 1984 which is also the current Swedish correction factor.

4.2.2 Current Correction Factor

In 1984 SGI decided, based on Helenelund's findings, to update the correction factor. The new correction factor was based on test results from normal consolidated clays with an overconsolidation ratio (OCR) of approximately 1.3.

The following empirical relation was established:

$$\mu = \left(\frac{0.43}{w_L}\right)^{0.45} \geq 0.5 \tag{4.1}$$

As one can observe from Figure 4.2 below, the new correction factor fitted well with Helenelund's findings. More importantly however, the new correction factor is more conservative than the original correction factor from 1969 and doesn't overestimate the shear strength from the shear vane test.

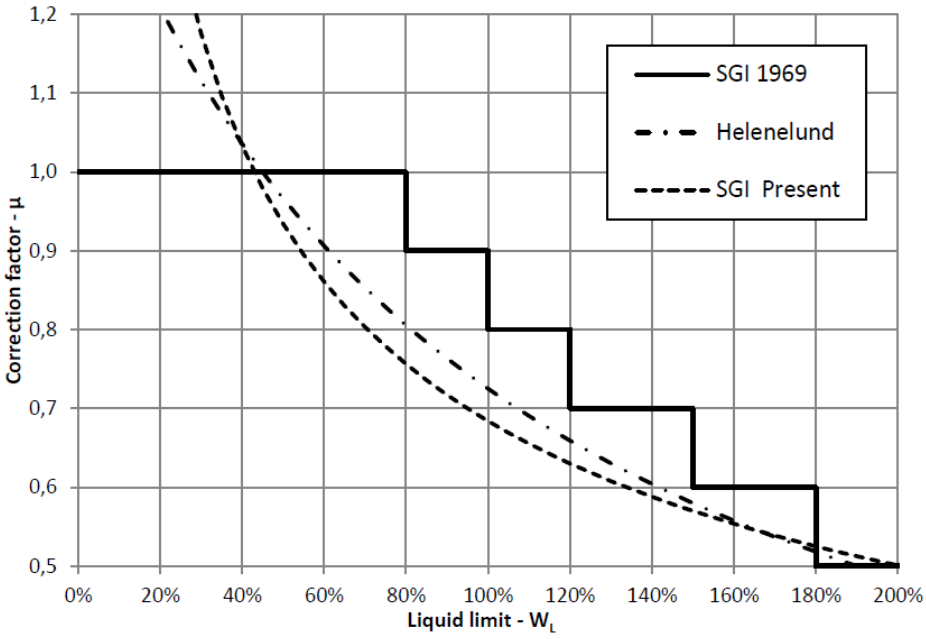

Figure 4.2: Swedish correction factors (after (Jonnson and Sellin, 2012))

In the meantime, the correction factor from 1984 has been revised, based on tests done by Larsson et al. (2007)), in order to make it applicable for over consolidated clays. As previously mentioned, the correction factor established in 1984 was based on tests on clays with an OCR of 1.3 (normal consolidated clays). The revised empirical relation :

$$\mu = \left(\frac{0.43}{w_L}\right)^{0.45} \left(\frac{OCR}{1.3}\right)^{-0.15} \tag{4.2}$$

The revised empirical relation is not only a function of the Atterberg liquid limit, but also the soil's stress history (in geotechnical terms over consolidation ratio).

Given an OCR of 1.3, the revised correction factor will be the identical to the correction factor established in 1984 which is reasonable as the original correction factor from 1984 was based on an OCR of 1.3.

4.3 Norwegian Correction Factors

4.3.1 Bjerrum's Correction Factor

Bjerrum (1972) porposed the first Norwegian correction factor. Using back calculations of known embankment failures, Bjerrum determined that each embankment's factor of safety was greater than 1, if they were based on the measured undrained shear strength from the shear vane test. His results were contradicting since the embankments had already failed.

This led to the introduction of the correction factor, to adjust the measured undrained shear strength. Bjerrum found a clear trend between factor of safety and plasticity index. In addition he believed that strain rate effects played a role. As one can observe from figure 4.3 below, Bjerum purposed two correction factors. One where only soil anisotropy was taken into account, the other one also factoring in strain rate effects.

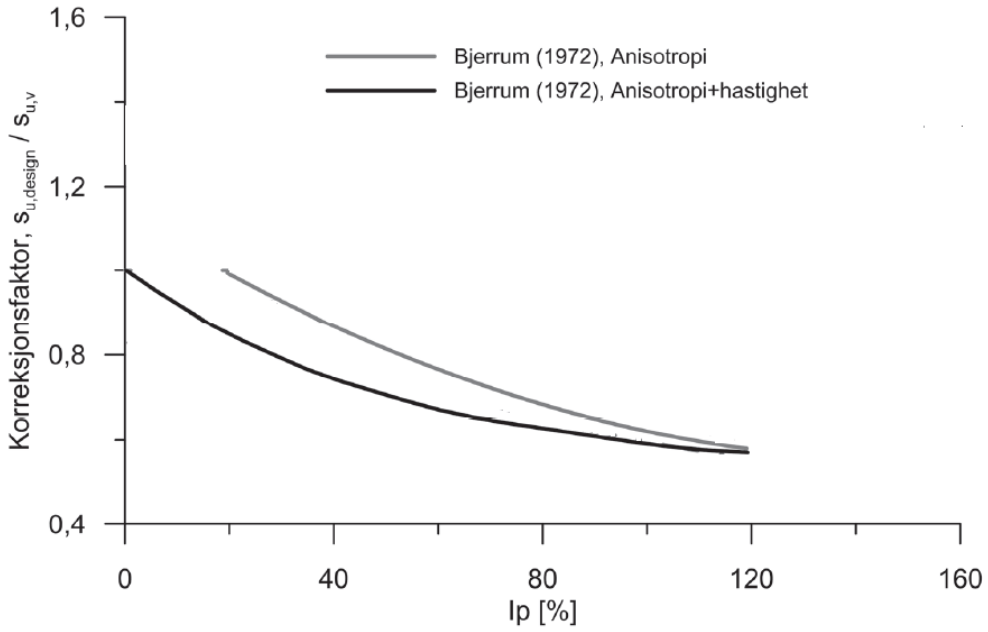

Figure 4.3: Bjerrum's correction factors (modified (NTNU, 2014))

Unlike the Swedish correction factors, the Norwegian correction factors are based on plasticity index. However the plasticity index is, like liquid limit, correlated to soil anisotropy. The greater the plasticity index, the more isotropic the soil is.

Bjerrum also factored in strain rate effects. Bjerrum stated that the effect of strain rate can also be described by the soil's plasticity index. The greater the plasticity index is,the greater the effect of strain rate is. Bjerrum didn't factor in progressive failure effects. He concluded that it only had a minimal effect, and therefore could be neglected.

4.3.2 Alternative Correction Factor

Aas (1979) proposed an alternative correction factor. Aas argued that over consolidation ratio is a better parameter than plasticity index when determining strain rate effects clays. Aas argued that strain rate effects are correlated to void ratio which is related to the soil's stress history (OCR). The greater the porosity of a soil (alternatively the less OCR is), the greater the effect of strain rate is. Aas' alternative correction factor:

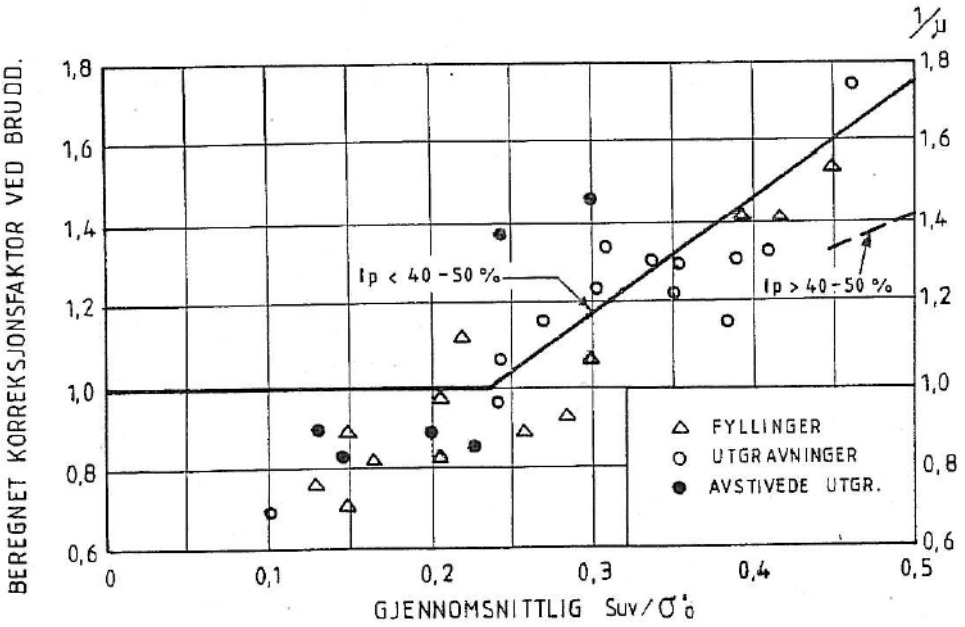

Figure 4.4: Aas' correction factor (after (Aas, 1979))

Part II

Numerical Analysis

In the second part of the report, 2D and 3D finite element method analysis of the shear vane test are performed. The software used is Plaxis 2D Version 2016.01 and Plaxis 3D Version AE.02. In Plaxis 2D 10 noded elements were used in plane strain. Meanwhile 10 noded elements were used in Plaxis 3D.

Numerical analysis were run to investigate to which extent progressive failure, strain rate and time effect and anisotropy aspects of material behavior affect the measured torque during the shear vane test.

Factors such as sample disturbance, waiting time, local drainage, local consolidation, heterogeneous soil and blade thickness will always be a factor when conducting the shear vane test and one should be aware that these factors will influence the measured torque. However these effects will not be further discussed in this report.

Chapter 5

Material Models

In this chapter a brief introduction and summary of each material model used in the numerical analysis will be given.

5.1 Mohr-Coulomb

The Mohr-Coulomb model is a simple, linear elastic perfectly plastic material model. It is often used as a first approximation of soil behavior. Within the yield surface the soil is linear elastic (all strains are reversible) based on Hooke's law of isotropic elasticity. The perfectly plastic region (irreversible strains) is based on the Mohr-Coloumb failure criteria, formulated in a non-associated plasticity framework. The model does not incorporate any time effects nor stress dependent parameters. (Plaxis, 2016)

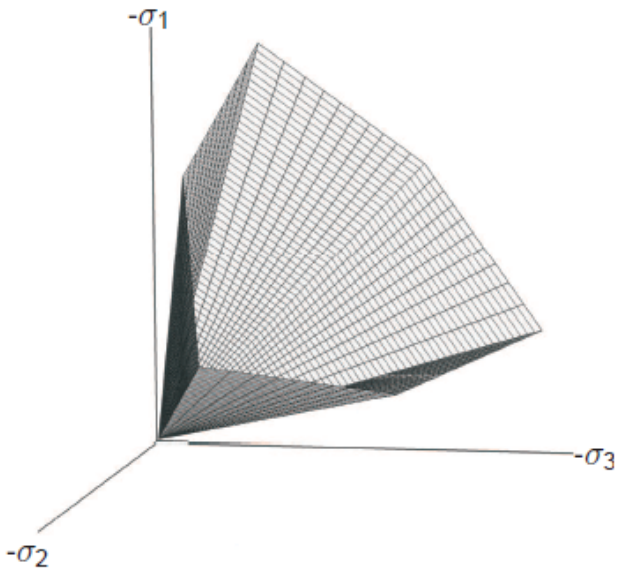

Figure 5.1: The Mohr-Coulomb yield surface in principal stress (c=0) (after (Plaxis, 2016)

The Mohr-Coulomb material model was used in the Plaxis 2D analysis in order to examine to which extent progressive failure (softening) affects the measured torque from the shear vane test. In addition the material model was used in the Plaxis 3D analysis in order to incorporate 3D effects.

Undrained A

Undrained effective stress analysis can be used in combination with effective strength parameters ϕ' and c' to model the material's undrained shear strength. In Plaxis this is referred to as Undrained(A) analysis. In this case, the development of the pore pressure plays a crucial role in providing the right effective stress path that leads to failure at a realistic value of undrained shear strength (s_u) (Plaxis, 2016) .

For a more thorough description of the Mohr-Coulomb model and Undrained(A) analysis, reference is made to Plaxis Material Models (Plaxis, 2016)

5.2 Geofuture Soft Clay

The Geofuture Soft Clay model is a user defined model developed by Ph.D candidate Jon Rønningen at NTNU. It is an effective stress based model for soft Scandinavian clays. The constitutive model is based on the theory of plasticity where concepts such as plastic flow and hardening rules are of fundamental importance. Unlike the Mohr-Coulomb model, time dependent parameters are introduced such that rate dependency, creep and relaxation can be modeled. (Rønningen, 2017)

The reference surface and the plastic potential can be represented by ellipsoids in principal stress space as shown in the Figure 5.2 and Figure 5.3.

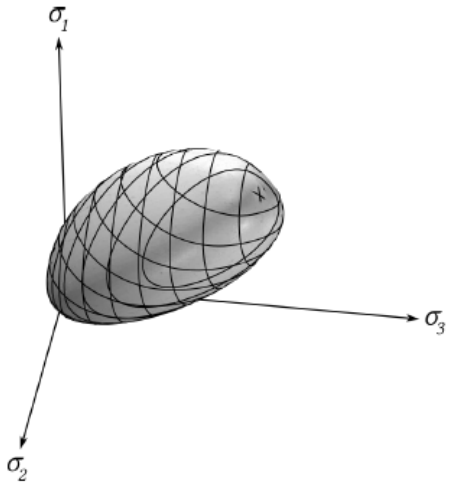

Figure 5.2: Reference surface in principal stress based (after (Rønningen, 2017))

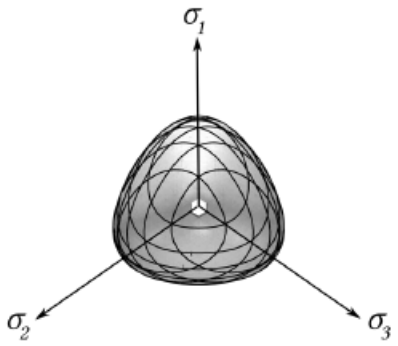

Figure 5.3: Reference surface in principal stress based (after (Rønningen, 2017))

The shape of the ellipsoids are typically corresponding to the Lade failure criterion in the deviatoric plane. The two surfaces have the ability to change their size, shape and orientation and may do so independently of each other, i.e. having the possibility of non associated flow. This allows features of natural soft or sensitive clays to be modeled, including anisotropy in strength and stiffness, unloading and reloading, destructuration and time dependence. (Rønningen, 2017)

For a more thorough description to the Geofuture Soft Clay Model, reference is made to the user manual.

The Geofuture Soft Clay constitutive model was applied in Plaxis 2D in order to examine strain rate effects and time effects during the shear vane test. It is commonly known that strain rate affects the measured undrained shear strength. As discussed in section 3.6, different time to failure yields different strain rates that in return result in different undrained shear strengths. The aim of the Geofuture Soft Clay analysis is to determine to which extent time effects affect the results during the vane test.

The Geofuture material model also incorporates soil anisotropy and softening aspects of soft clay material behavior (in addition to time effects). However softening and anisotropy will in this report not be investigated using the Geofuture material model.

5.3 NGI ADP

The NGI ADP model is a material model that factors in anisotropic properties of clays. Unlike the Geofuture material model, NGI ADP is a total stressed based material model.. As written in the Plaxis Material Model manual (Plaxis, 2016), the basis of the model is:

- Input parameters for undrained shear strength for three different stress paths/states (Active, Direct Simple Shear and Passive).
- A yield criterion based on a translated approximated Tresca criterion.
- Elliptical interpolation functions for plastic failure strains and for shear strengths in arbitrary stress paths.
- Isotropic elasticity given by unloading/reloading shear modulus, G_{ur}.

The failure criterion of the NGI ADP model can be observed below:

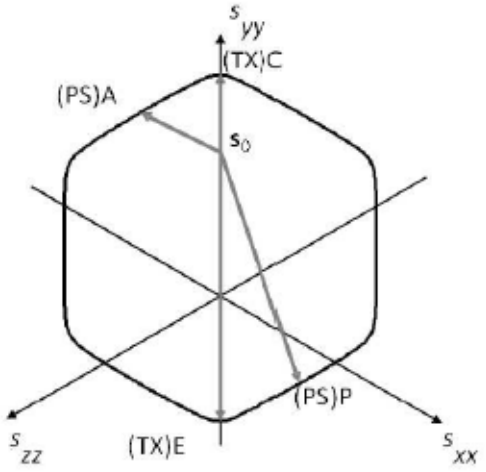

Figure 5.4: Failure criterion of the NGI ADP model in the π plane (after (Plaxis, 2016))

For a more thorough description of the NGI ADP model, reference is made to the Plaxis Material Model Manual (Plaxis, 2016).

The NGI ADP material model was applied in Plaxis 3D in order to investigate the effect of anisotropy on the measured torque from the shear vane test. It is commonly known that any form of anisotropy affects the results during the shear vane test. As previously mentioned, anisotropy is the main reason for the correction factors mentioned in Chapter 4. The aim of the Plaxis 3D simulations using the NGI ADP model is to determine to which extent anisotropy affects the measured torque from the shear vane test.

Chapter 6

Model and Material Parameters

6.1 Geometry

The geometry used in the numerical simulations is based on the standard vane used in Norway. The standard vane has a diameter of 55mm and a height of 110mm. In Plaxis it was necessary to create a large enough soil contour so that the boundary surfaces would not affect the results from the numerical simulations.

In Plaxis 2D a 200mm by 200 mm soil box was modeled. Meanwhile in Plaxis 3D a soil cube of 400mm by 400mm by 400mm was modeled. The input parameters not mentioned in this chapter are defined by the default settings in Plaxis.

6.2 Material Parameters

The values of each material parameter (input parameter) for every material model were decided in collaboration with Ph.D Candidate Jon Rønningen. The values of each material parameter were based on typical values for soft Norwegian clays.

6.2.1 Mohr-Coulomb

The Mohr-Coulomb material parameters are summarized in Table 6.1. The Mohr-Coulomb material parameters are identical in the 2D and 3D simulations.

Table 6.1: Mohr Coulomb material parameters

Material Model	Mohr-Coulomb
Drainage Type	Undrained A
Soil Weight, γ	0 $\frac{kN}{m^4}$
Stifness, E$^{'}$	10 MPa
$\nu^{'}(nu)$	$\frac{1}{3}$
Cohesion, $c^{'}_{ref}$	5 kPa
Friction Angle, θ	20
Dilatency Angle	-1

A negative dilatency angle was chosen to examine the effect of softening and progressive failure when executing the shear vane test.

6.2.2 Geofuture Soft Clay

The input parameters of the Geofuture Soft Clay model are shown below:

Table 6.2: Geofuture Soft Clay input parameters

		Parameters
1	$\frac{G_{ur}}{\sigma_{y,0}}$	Normalized Shear Stiffness
2	m_{nc}	The Janbu (nc) Oedometer Modulus
3	m_{oc}	The Janbu (oc) Oedometer Modulus
4	r_{si}	The instristic Janbu Creep Modulus
5	$s^{TXC}_{20\%}$	Ratio between undrained shear strength at peak and at 20 % strain in triaxial compression for a given strain rate and OCR
6	$\frac{s^{TXC}_u}{\sigma_{y,0}}$	Normalized undrained shear strength in triaxial compression for a given strain rate and OCR
7	$\frac{s^{TXE}_u}{s^{TXC}_u}$	Ratio between undrained shear strength in triaxial extension and compression at a given strain rate and OCR
8	$\frac{\Delta\epsilon_y}{\Delta t}\Big\vert_{s_u}$	The strain rate for which the inputs above are given (per day)
9	ϕ_{cs}	Friction angle (corresponding to Lade's failure criteria)
10	K^{NC}_0	Asymptotic ratio between horizontal and vertical effective stress in an oedometer
11	OCR	Degree of over-consolidation

The values chosen for each input parameter can be observed in the table below:

Table 6.3: Geofuture Soft Clay material parameters

		Parameters
1	$\frac{G_{ur}}{\sigma_{y,0}}$	70
2	m_{nc}	20
3	m_{oc}	100
4	r_{si}	500
5	$\mathrm{s}_{20\%}^{TXC}$	0.7
6	$\frac{s_u^{TXC}}{\sigma_{y,0}}$	0.35
7	$\frac{s_u^{TXE}}{s_u^{TXC}}$	0.4
8	$\frac{\Delta\epsilon_y}{\Delta t}\Big\vert_{s_u}$	0.1
9	ϕ_{cs}	28
10	K_0^{NC}	0.6
11	OCR	1.2

All input parameters remained constant for all simulations. However a different time to failure was chosen for each simulation. The time to failure varied from 1 minute, 3 minutes, 1 hour, 3 hours and 1 day.

1 minute and 3 minutes were chosen as these are respectively the lower and upper bounds of the standard time during the shear vane test. 1 hour, 3 hour and 1 day were chosen as these are plausible values of time to failure during a laboratory test.

The degree of anisotropy and softening of the soil for each simulation stayed constant. In that way, the difference in the results of each simulation are due to different strain rates.

6.2.3 NGI ADP

The input parameters of the NGI ADP model are shown below:

Table 6.4: NGI ADP input parameters

Parameter	Description
$\frac{G_{ur}}{s_u^A}$	Ratio unloading/reloading shear modulus over (plane strain) active shear strength
γ_f^C (%)	Shear strain at failure in tri-axial compression
γ_f^E (%)	Shear strain at failure in tri-axial extension
γ_f^{DSS} (%)	Shear strain at failure in direct simple shear
$s_{u,ref}^A$	Reference (plane strain) active shear strength
$\frac{s_u^{C,TX}}{s_u^A}$	Ratio tri-axial compression shear strength over (plane strain) active shear strength
y_{ref}	Reference depth
$s_{u,inc}^A$	Increase of shear strength with depth
$\frac{s_u^P}{s_u^A}$	Ratio of (plane strain) passive shear strength over (plane strain) active shear strength
$\frac{\tau_0}{s_u^A}$	Initial mobilization
$\frac{s_u^{DSS}}{s_u^A}$	Ratio of (plane strain) direct simple shear strength over (plane strain) active shear strength

All parameters were kept constant for each simulation except for $\frac{s_u^{DSS}}{s_u^A}$ and $\frac{s_u^P}{s_u^A}$. The two parameters were manipulated for each simulation in order to investigate the effect of anisotropy. The active shear strength (s_u^A) was constant for every simulation.

The value for each parameter can be observed below:

Table 6.5: NGI ADP material parameters

Parameter	Description
$\frac{G_{ur}}{s_u^A}$	600
γ_f^C (%)	2
γ_f^E (%)	5
γ_f^{DSS} (%)	4
$s_{u,ref}^A$	10 kPa
$\frac{s_u^{C,TX}}{s_u^A}$	0.99 (default)
y_{ref}	0
$s_{u,inc}^A$	0
$\frac{s_u^P}{s_u^A}$	*
$\frac{\tau_0}{s_u^A}$	0.7 (default)
$\frac{s_u^{DSS}}{s_u^A}$	*

$*$ varied for each simulation

The values of $\frac{s_u^{DSS}}{s_u^A}$ and $\frac{s_u^P}{s_u^A}$ for each simulation where based on the findings of Thakur (2013). Thakur (2013) found the following empirical relations for Norwegian Clay

Table 6.6: Correlation between anisotropy and plasticity index (After (Thakur, 2013))

$\frac{s_u^{DSS}}{s_u^A}$	$\frac{s_u^P}{s_u^A}$
0.63 +0.00425·$(I_p - 10)$	0.35 +0.00375·$(I_p - 10)$

In total 6 simulations with 6 different plasticity indexes were run to investigate effect of anisotropy during the shear vane test.

Table 6.7: Values for each simulation using the NGI ADP model

Simulation	I_p	$\frac{s_u^{DSS}}{s_u^A}$	$\frac{s_u^P}{s_u^A}$
1	10	0.63	0.35
2	20	0.6725	0.3875
3	30	0.715	0.425
4	40	0.7575	0.4625
5	50	0.8	0.5
6	90	0.97	0.65

6.2.4 Vane Blades

Typical values of steel were chosen for the material parameters of the vane blades.

Table 6.8: Vane blade material parameters

EA_1	$12 \cdot 10^6$
EA_2	$12 \cdot 10^6$
EI	$65.4 \cdot 10^3$
$\nu(nu)$	0.499

The material parameters in the table above were kept constant for every simulation. In the 2D simulations a zero thickness vane was used. Meanwhile blades of thickness 1 m were applied in the 3D simulations to ensure a rigid vane.

6.3 Plaxis 2D

The model, mesh and calculation steps in Plaxis 2D were kept identical, independent of the material model applied.

6.3.1 Model

The following Plaxis model,with contours $X_{min} = 0.0m$, $X_{max} = 0.2m$, $Y_{min} = 0.0m$ and $Y_{max} = 0.2m$, was used for the numerical 2D analysis:

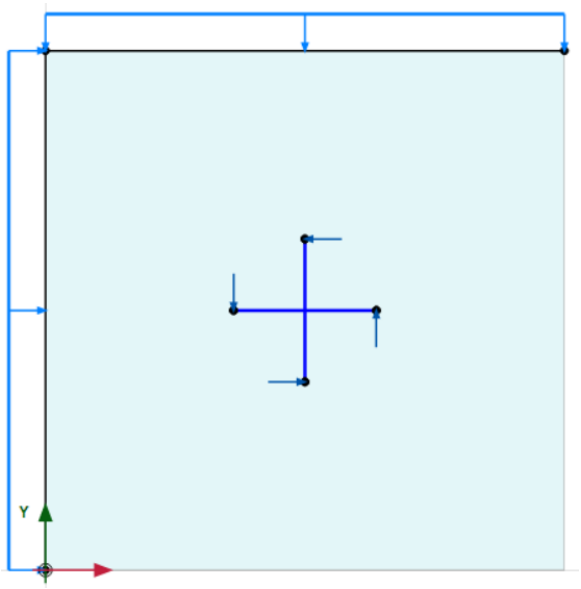

Figure 6.1: Plaxis 2D model

Initially there were some issues regarding modeling the vane test. Conventionally, Plaxis 2D is used to model vertical sections (vertical planes). However in this model one is interested in modeling a horizontal section.

Modeling a horizontal section was achieved by setting γ to 0 and applying line load which represented horizontal stresses on the left and upper boundaries . In this manner a uniform stress state was achieved. A uniform stress state represents a horizontal section.

In Plaxis it is not possible to apply constant rotation as displacements. Therefore it was necessary to apply a point load at each tip of the vane to simulate the torque that the vane experiences during the vane test. These point loads were gradually increased until failure during the numerical analysis using multipliers.

6.3.2 Mesh

A fine mesh consisting of 2983 elements was used. In order to achieve a finer mesh around the vane, a coarseness factor of 0.5 was applied around the vane. The mesh can be observed in Figure 6.2 below.

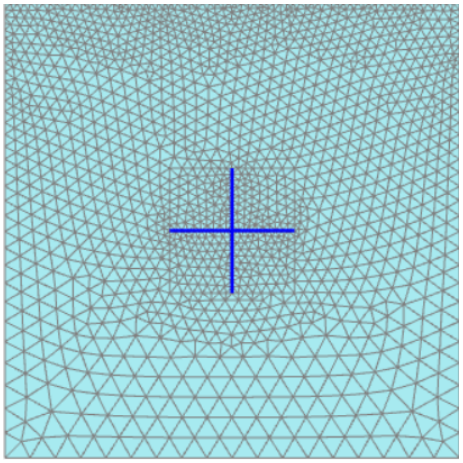

Figure 6.2: Plaxis 2D mesh

6.3.3 Calculation steps

In total three phases were created to simulate the shear vane test; initial phase, second phase and third phase.

Initial Phase

The model during the first phase can be observed in Figure 6.3 below.

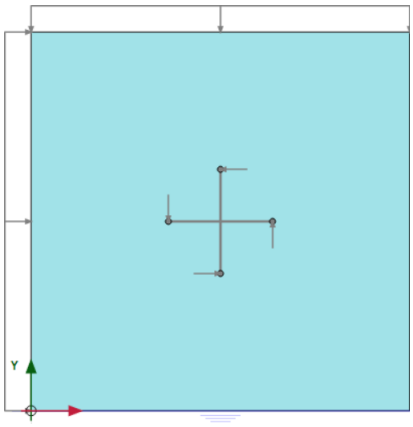

Figure 6.3: First phase

Due to the weightless soil, the soil doesn't experience any load during the first phase. The first phase does not represent a real situation (weightless soil and no load). The initial phase

is only there for practical purposes in Plaxis. Neither the vane, the line loads nor the point loads are activated.

Second Phase

The model during the second phase can be observed in figure 6.4 below.

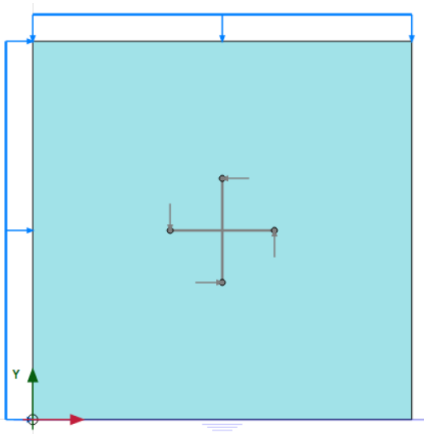

Figure 6.4: Second phase

In the second phase the line loads of 100 kPa on the left and upper boundary are activated. Due to the weightless soil in the model, the stresses on the left and upper boundary are to represent stresses caused by the weight of the soil itself at a certain depth (a depth equivalent of 100 kPa). In this phase, a uniform stress state is achieved, which is the case in a horizontal section of a soil.

In addition undrained behavior is ignored in order to avoid any excess pore pressure being developed when activating the horizontal stresses. Since these horizontal stresses are permanent, one does not want any excess pore pressure to build up when activating the stresses in Plaxis.

Third phase

The soil model during the third phase can be observed in figure 6.5 below.

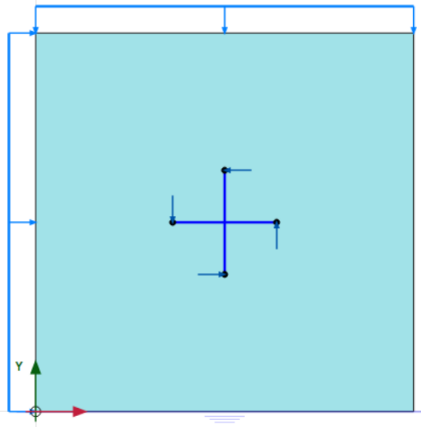

Figure 6.5: Third Phase

The last phase represents the execution of the shear vane test. Initially, the displacements from the second phase are reset to zero.

The point loads of 20 kN and the shear vane are activated. By activating the point loads, a torque is achieved. In Plaxis the point loads (and the resulting torque) are incrementally increased until the soil fails.

6.4 Plaxis 3D

The model, mesh and calculation steps in Plaxis 3D were kept identical, independent of the material model applied.

6.4.1 Model

A Plaxis model (Figure 6.6), with contours $X_{min} = -0.2m$, $X_{max} = 0.2m$, $Y_{min} = -0.2m$ and $Y_{max} = 0.2m$, was used for the 3D numerical analysis.

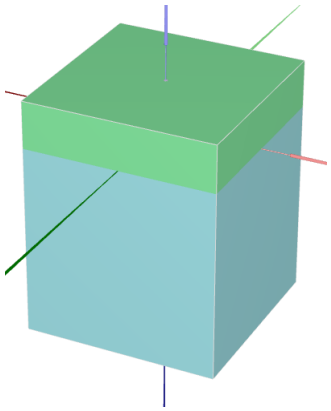

Figure 6.6: Soil box in Plaxis 3D

The thickness of the green and blue layers are 0.1m and 0.4 m respectively. The green layer was added in order to create an initial uniform state of stress of 100 kPa. A uniform state of stress was achieved by setting the unit weight of the green layer to 1000 $\frac{kN}{m^3}$ and K_0 to 1. By having identical initial stress (100kPa) in the 2D and 3D simulations, one can easily compare the results from the respective simulations.

The model of the shear vane in Plaxis 3D can be observed below:

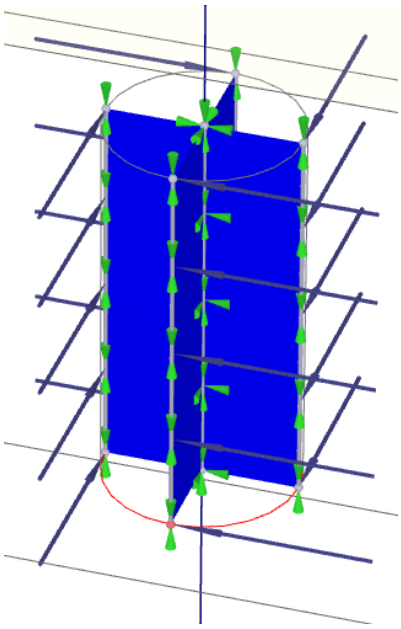

Figure 6.7: Shear vane in Plaxis 3D

Torque was simulated by applying line loads at the end of each blade. Initially there were some problems regarding the rotation of the vane. Correct rotation of the vane was ensured by creating line displacements at the tip of each blade and at the center of the vane. Each tip was fixed in the x and y direction and free in the z direction. The center of the vane was fixed in the x,y and z direction.

6.4.2 Mesh

The mesh consists of 34436 elements. In order to achieve a finer mesh around the vane and the surrounding soil which is remolded during the vane test, a cylinder was created. The coarseness factor of the cylinder was set to 0.5. The coarseness factor of the boundaries of the soil box was set to 8 in order to decrease calculation time.

The mesh at the soil boundaries, the cylinder and the vane are shown Figure 6.8, Figure 6.9 and Figure 6.10 below:

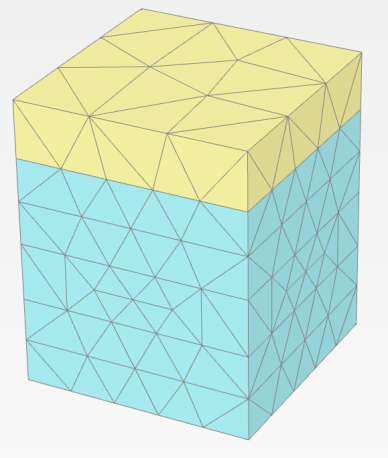

Figure 6.8: Soil boundary mesh

As one can observed the mesh is very coarse at the boundaries. This is to reduce calculation time. The measured torque was independent of the mesh at the boundaries.

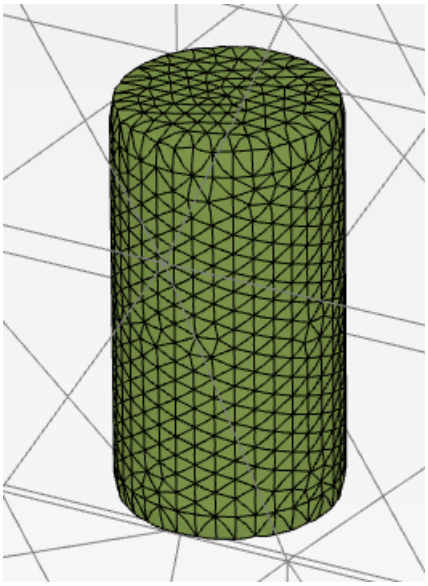

Figure 6.9: Cylinder mesh

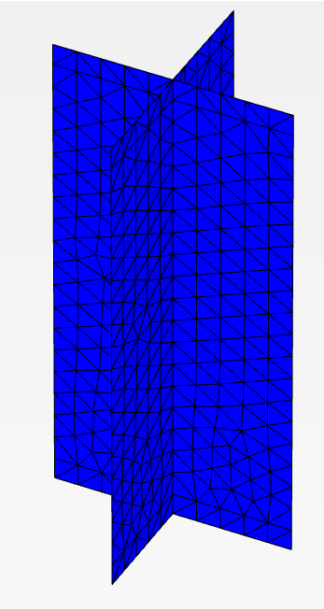

Figure 6.10: Vane mesh

The mesh is finer around the cylinder and the vane.

6.4.3 Calculation Steps

Initial Phase

In the initial phase, the soil only is loaded with its own weight. Since the second layer (blue layer) is weightless, there is a uniform state of stress through the entire blue layer.

Second Phase

The vane, line displacements on the vane and the line loads at the tip of each vane are activated. By activating the line loads the shear vane test is simulated.

Chapter 7

Results and Discussion

In the following chapter, the results from numerical simulations in addition to hand calculations will be presented and discussed. Numerical analyses were run to investigate to which extent progressive failure (softening), strain rates and anisotropy aspects of cohesive soil behavior influence the results in the shear vane test.

7.1 Hand Calculations

In order to validate the results from the Plaxis 2D and 3D simulations, simple hand calculations are computed to determine approximately the magnitude of the torque at failure to expect from the numerical simulations. In the hand calculations an isotropic soil is assumed. This implies that the strength on the vertical and horizontal surfaces are identical (s_{uh}=s_{uv}).

Before any calculations are made the general equation for torque is derived.

By definition, torque is defined as

$$T = Force \cdot lever\ arm$$

.
Force can also be expressed as:

$$\int_A Stress \cdot dA$$

where A is Area.

Thus, torque can be expressed as:

$$\int_A Stress \cdot dA \cdot Lever\ arm$$

For the hand calculations, the radius and height of the vane are defined as r and H respectively.

The hand calculations are based on the conventionally assumed failure geometry below (discussed in section 2.3).

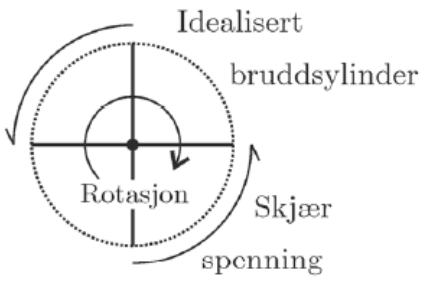

Figure 7.1: Assumed geometry of the failure surface (NTNU, 2014)

In order to calculate the theoretical solution, the undrained shear strength must be determined. The undrained shear strength of the soil is found by running a direct shear stress test in Plaxis SoilTest. The soil is identical to the soil run in the Mohr-Coulomb Plaxis simulations. In the direct stress stress test, the initial stress was set to 100 kPa (which corresponds to the confining stress in the Plaxis 2D and 3D simulations).

The results from the test can be observed below in figure 7.2.

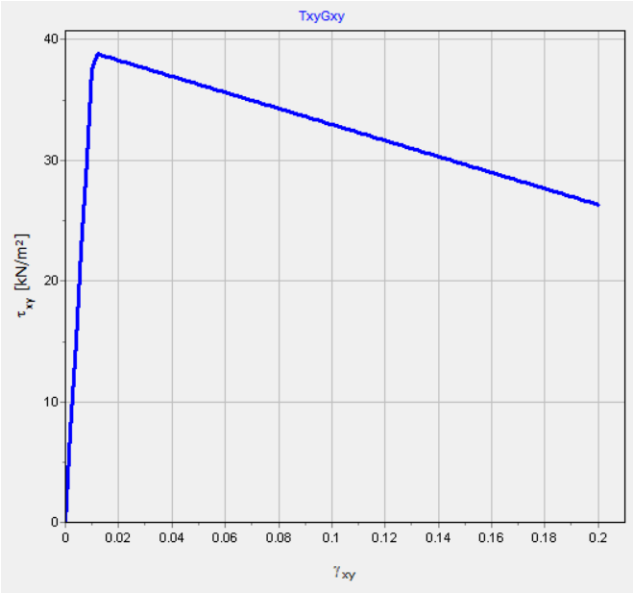

Figure 7.2: Direct simple shear test in Plaxis SoilTest

From the graph one can observe a peak undrained direct shear strength of 39 kPa.

7.1.1 2D Hand Calculation

For the Plaxis 2D simulations, all 3D effects are neglected. As a consequence the torque in the horizontal planes are neglected. Only the vertical torque contributes to the total torque. By following the equation derived above;

$$T = \int_A Stress \cdot dA \cdot Lever\ arm$$

then the torque at failure in 2D will be given as

$$T_{total} = T_{vertical} = s_u \cdot (2\pi \cdot r \cdot H) \cdot r$$

where

- s_u is the resistance(stress) of the fully mobilized soil
- $2\pi \cdot r \cdot H$ is the total area
- r is the lever arm

As a result of the height to diameter ratio of the shear vane being 2:1 (alternatively height to radius ratio of 4:1), the f

$$T_{total} = s_u \cdot (2\pi \cdot r \cdot 4r) \cdot r$$

thus

$$T_{total} = s_u \cdot 8\pi \cdot r^3$$

Now that all variables are known, one can simply determine the torque at failure by inserting each variable in the formula derived above:

$$T_{total} = s_u \cdot 8\pi \cdot r^3$$

$$T_{total} = 39kPa \cdot 8\pi \cdot (0.0275m)^3$$

$$T_{total} = 20.38Nm$$

+

7.1.2 3D Hand Calculation

In the Plaxis 3D simulation, 3D effects are incorporated. In the shear vane test this implies that the the horizontal planes contribute to the total torque. In 3D the total torque consists of a vertical and horizontal component.

As derived in the subsection 7.1.1 above , the torque on the vertical surface is

$$T_{vertical} = s_u \cdot 8\pi \cdot r^3$$

In addition to the moment on the vertical surface, the moment on top and buttom horizontal surfaces of the vane contributes to the total torque. By following the equation derived above;

$$T = \int_A Stress \cdot dA \cdot Lever\ arm$$

then the contribution of one horizontal surface is

$$T = 2 \cdot \int_0^r s_u \cdot \pi r^2 \cdot dr$$

- 2 is due to symmetry of the failure circle
- s_u is the resistance of the soil
- πr^2 is the area
- dr is the lever arm

Solving the integral gives the total torque on one horizontal surface

$$T = 2 \cdot \pi \cdot s_u \int_0^r r^2 \cdot dr$$

$$T = 2 \cdot \pi \cdot s_u \cdot \frac{r^3}{3}\Big|_0^r$$

$$T = \frac{2}{3} \cdot \pi \cdot s_u \cdot r^3$$

Due to two horizontal surfaces (on top and on buttom of the vane) the total torque on both horizontal surfaces is

$$T = \frac{4}{3} \cdot \pi \cdot s_u \cdot r^3$$

Thus the total torque in 3D is

$$T_{total} = T_{horizontal} + T_{vertical}$$

$$T_{total} = \frac{4}{3} \cdot \pi \cdot s_u \cdot r^3 + s_u \cdot 8\pi \cdot r^3$$

$$T_{total} = \frac{28}{3} \cdot \pi \cdot s_u \cdot r^3$$

Alternatively, if r can be replaced with $\frac{D}{2}$.

Then

$$T_{total} = \frac{7}{6} \cdot \pi \cdot s_u \cdot D^3$$

By inserting the values of each parameter,

$$T_{total} = \frac{28}{3} \cdot \pi \cdot 39kPa \cdot (0.0275m)^3$$

$$T_{total} = 23.78Nm$$

As one can observe; the total torque in 3D is greater than in 2D due to the contribution of the horizontal surfaces. However, the contribution of the horizontal surfaces are not as significant as the one from the vertical surface. 85.7 % of the total torque is due to the vertical surface.

$$\frac{T_{vertical}}{T_{total}} = \frac{8 \cdot \pi \cdot s_u \cdot r^3}{\frac{28}{3} \cdot \pi \cdot s_u \cdot r^3} = \frac{6}{7} \approx 0.857$$

7.2 Mohr-Coulomb Plaxis 2D

7.2.1 Torque at Failure

From the Plaxis simulation, the torque at failure can be determined using the following equation:

$$T_{Plaxis} = 4 \cdot F \cdot M_{stage} \cdot r \cdot H$$

where

- 4= number of point loads
- F= Force applied at each point load
- M_{stage}= step multiplier
- r= Radius of the vane
- H=Height of the vane

As previously mentioned, a force of 20kN/m was applied to the end of each blade. The vane failed at a M_{stage} value of 0.081.Thus the torque at failure is:

$$T_{Plaxis} = 4 \cdot 20kN/m \cdot 0.081 \cdot 0.0275m \cdot 0.11m$$

$$T_{Plaxis} = 19.6Nm$$

The torque at failure from the Plaxis simulation is similar to the result from the hand calculation (19.6 Nm and 20.38 Nm respectively). Percent differnce:

$$\left| \frac{19.6Nm - 20.38Nm}{20.38Nm} \right| \cdot 100\% = 3.8\%$$

7.2.2 Deformed Vane

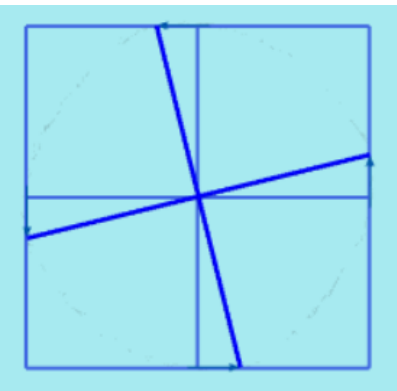

Figure 7.3: Deformed vane

The deformation of the vane seem to fit well with shear vane theory. The center of the vane is stayed put, the vane experiences a rotation that is equal for all four rectangular plates (in this case each plate experiences a rotation of 1.402°). The vane can be considered rigid (no relative deformation) as a result of its stiffness being many magnitudes greater than the stiffness of the adjacent soil.

7.2.3 Direct Simple Shear Strength and Failure Mode

In order to determine which failure mode (active,passive or direct) the shear vane test simulates in a horizontal plane, it is necessary to determine the strength from the numerical simulations.

To determine the undrained shear strength from the Plaxis simulation, deviatoric stress was plotted with respect to shear strains. The deviatoric stress-deviatoric strain plot can be observed below:

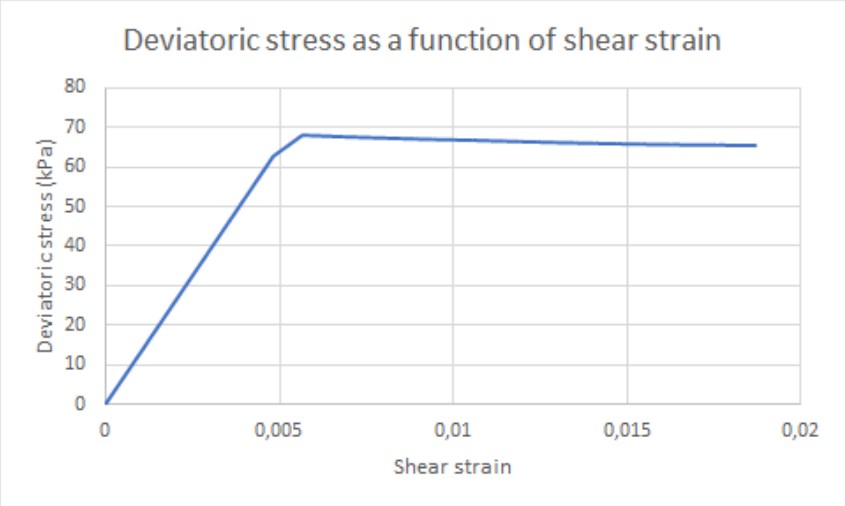

Figure 7.4: Deviatoric stress- shear strain plot

As one can observe, the peak deviatoric stress is approximately 68 kPa. A post peak softening behavior is present. At a shear strain of 1.5 per cent the deviatoric stress is 95 per cent of the peak strength.

Chandler (1988) argued that the vane test simulates a direct simple shear test in a horizontal plane. If one assumes that it is correct, then the undrained shear strength can be determine by the following relation:

$$\tau = s_u = \frac{q}{\sqrt{3}}$$

where q is the deviatoric stress.

The relation above is based on the Von Mises yield criteria for a case of pure shear. In this simulation the peak deviatoric stress was 68 kPa, thus the peak shear stress is:

$$\tau = s_u = \frac{68}{\sqrt{3}} = 39kPa$$

An undrained shear strength of 39 kPa is precisely the undrained shear strength found from Plaxis Soil Test when running a direct shear test (figure 7.2).

The numerical simulations seem to indicate that the thesis proposed by Chandler (1988) is correct when using the Mohr-Coulomb material model. He argued that the shear vane simulates a direct simple shear stress in a horizontal section.

7.2.4 Incremental strains

The four figures below show chronological the development of deviatoric strains during the vane test.

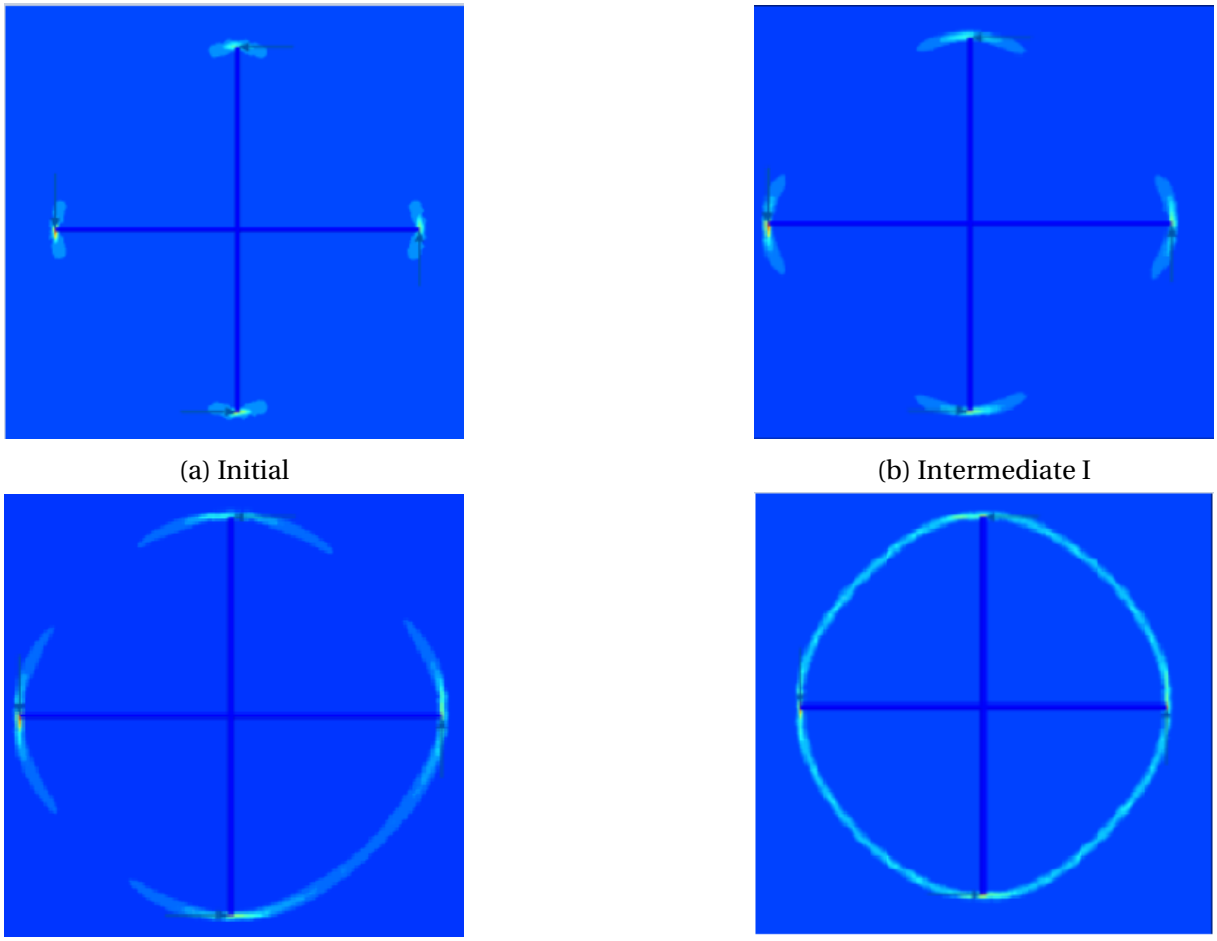

(a) Initial

(b) Intermediate I

(c) Intermediate II

(d) Final

Figure 7.5: Incremental strains

Figure 7.5 shows the development of the failure zone. As one can observe, the circular like shape of the failure mode is more or less constant throughout steps a to d. However the failure zone increases as the load is incrementally increased during the Plaxis simulation. One can observe that the zone around each blade edge goes to failure first.

Oddly, figure (c) shows a asymmetrical failure shape. It is not necessarily due to material behavior, but rather seems to be a result of an asymmetrical mesh.

Due to the softening behavior of the soil the failure mode is, as discussed in section 3.5, not entirely circular but rather a more square-rounded shape. A non-softening clay, with a dilatency angle of 0, would exhibit a perfectly circular failure mode as the one showed in figure 7.6 below.

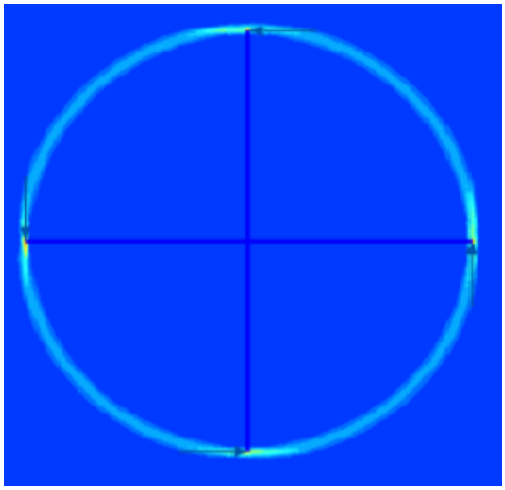

Figure 7.6: Failure mode when $\psi = 0$

The results from the numerical analysis seems to suggest that the softening behavior does have an impact of the failure shape. A softening material has a square-rounded failure surface while a non-softening material with ψ=0 has a circular shape.

Due to similar results of the torque at failure from hand-calculation (where progressive behavior wasn't taken into account) and the Plaxis simulations (where progressive behavior was taken into account) it seems to indicate that the progressive failure (softening) aspect of material behavior can be neglected when using a Mohr-Coulomb material model. However, more analysis should be conducted.

7.2.5 Further Mohr-Coulomb 2D Analysis

In the following section, the results from the numerical simulation are discussed in more detail. The discussion is based on the results from the Plaxis simulation and Figure 7.7 .

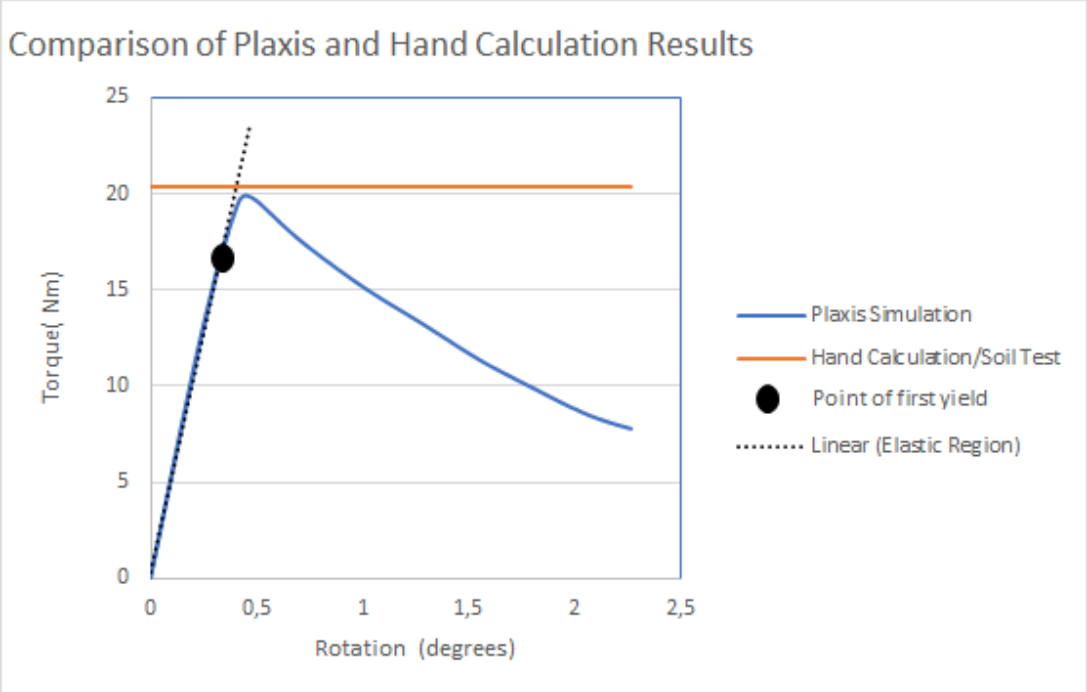

Figure 7.7: Plaxis SoilTest vs Plaxis comparison

In Figure 7.7 above, torque is plotted with respect to rotation.

As the vane only experiences relative small rotations, rotation is defined as displacement of the vane divided by radius of the vane. This assumption is valid, as $\sin\phi \cong \phi$ when $\phi \leq 5$ degrees. The torque from the Plaxis simulation is calculated, by the definition introduced in subsection 7.2.1:

$$T = 4 \cdot F \cdot M_{stage} \cdot R \cdot H$$

Plaxis SoilTest (which is used for the hand calculations) doesn't give displacement nor rotation as an output. Therefore it is not possible to plot the SoilTest curve with respect to rotation. However one knows, from the 2D hand calculation previously done (subsection 7.1.1), that the torque at failure is 20.38 Nm. This value is plotted to compare it to the value from the Plaxis simulation.

As one can observe in Figure 7.7, the torque from the Plaxis simulation decreases after reaching its peak value. This is due to the negative dilatency angle. Furthermore it should be noted that, due to the negative dilatency angle, the SoilTest curve will also show a post peak soft-

ening behavior. However, this is however not plotted as exact values of post peak torque and rotations values are unknown.

A negative dilatency angle of -1 was chosen, as a greater values often leads to numerical issues. If a dilatency angle of 0 was chosen, then the torque would be constant until failure after reaching its peak value.

Effect of Progressive Failure

The most interesting note regarding Figure 7.7 is that it seems to indicate the lack of role the effect of progressive failure plays in the shear vane test when using the Mohr-Coulomb material mode. In the Plaxis simulation, the softening behavior of the soil (and thus progressive failure) is taken into account when determining the capacity of the vane since the load at each end of the vane is added incrementally. However, in the hand calculation one assumes the the soil along the failure surface is fully mobilized simultaneously (non-progressive failure).

As one can observe, the peak torques are almost equivalent (percent difference of 3.8 %). The numerical simulations suggests that the effect of progressive failure can be neglected. In a progressive failure, like the one in the Plaxis simulation, the mobilized resistance along the failure surface will be smaller than the sum of the peak strengths in the extension, compression and direct zone. This is also the case in figure 7.7. The peak torque in the progressive failure (numerical simulation) is indeed smaller than the peak torque in the non-progressive failure (hand calculation), albeit not by much.

This finding, which seems to indicate that effect of progressive failure can be ignored, seems to confirm the finding from Cadling and Odenstad (1948). In their research they found the effect of progressive failure to be minimal and could therefore be neglected.

Linear Elastic, non-perfect Plastic Material

As theory says, the soil initially follows linear-elastic theory until the point of first yield (the black point in figure 7.7). From that point on, the soil goes into the plastic region. Due to the negative dilatency angle,the soil is not perfectly plastic.

In the linear-elastic region there is a linear relationship between force and displacement. Due to a linear relationship between torque & force, and rotation & displacement, there is therefore also a linear relationship between torque and rotation. This linear relationship can

be observed in the elastic region in the diagram. Linear elastic implies a constant stiffness in the elastic region.

Effect of the Soil Stiffness

In order to determine the effect of the stiffness of the soil, two additional simulation were run in which the stiffness varied from 1 MPa (soft clay) to 100 MPa (very stiff clay). These two simulations were compared to the original simulation done previously in this chapter where the stiffness was set to 10 MPa (medium stiff clay).

No matter the stiffness of the soil, the force applied at failure and thus torque at failure remained the same. A constant torque at failure means that the capacity of the soil is independent of its stiffness. However, the displacement and the rotation the vane experienced was inversely proportional with the stiffness of the soil. The stiffer the soil was, the less displacement/rotation the vane experienced. The displacement and rotation values for each stiffness is summarized in the table below:

Table 7.1: Displacement and rotations of the vane for different stiffness values

Stiffness,$E^{'}$ (MPa)	Displacement (mm)	Rotation (degrees)
1	2.36	4.84
10	0.236	0.484
100	0.023	0.0478

An one can observe from the table, a ten fold increase in stiffness, decreases the displacement and rotation by a ten fold.

Regardless of the stiffness of the soil, the vane stayed rigid (no relative displacements) due to its high stiffness. The stiffness of the vane is much greater than the stifness of the soil. Typically the stiffness of the vane (steel) is 210 GPa thus stiffness of the soil has little or no effect of the stiffness of the entire system.

To validate the Plaxis simulation results, Plaxis soil tests were conducted :

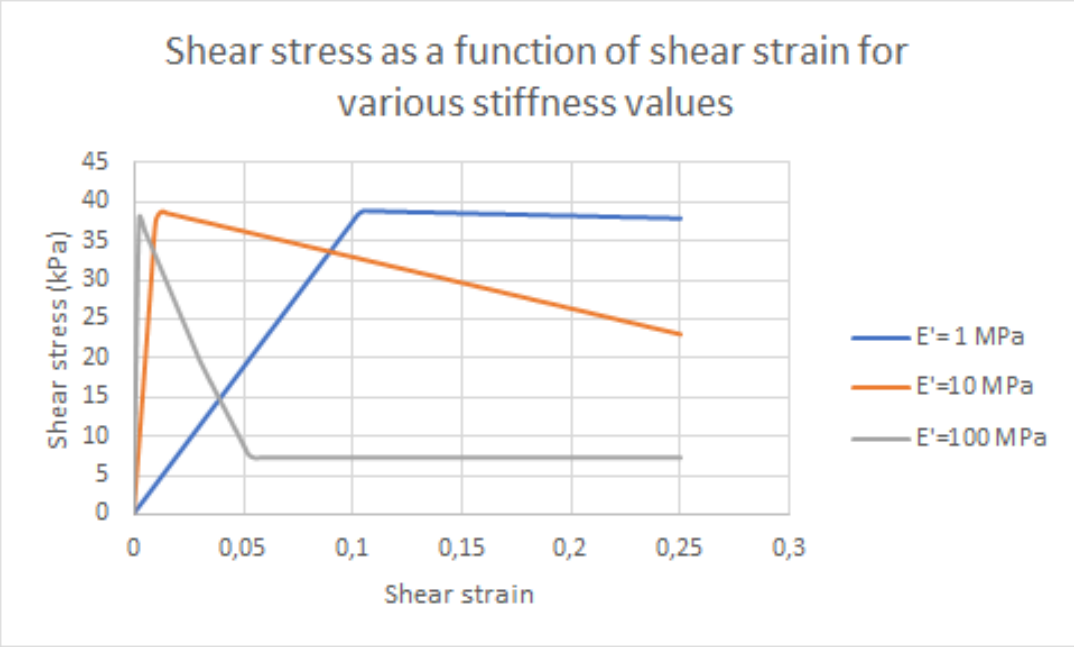

Figure 7.8: Displacements and rotations of the vane for different stiffness values

The peak undrained shear strength is, shown in Figure 7.8 above, independent of the stiffness of the soil. A constant peak undrained shear strength implies that the torque at failure is constant regardless of the stiffness of the soil. This fits well with the results from the Plaxis simulation.

7.3 Geofuture Soft Clay-Plaxis 2D

7.3.1 Torque at Failure

For each simulation the torque was determined by the same formula previously used:

$$T = 4 \cdot F \cdot M_{stage} \cdot R \cdot H$$

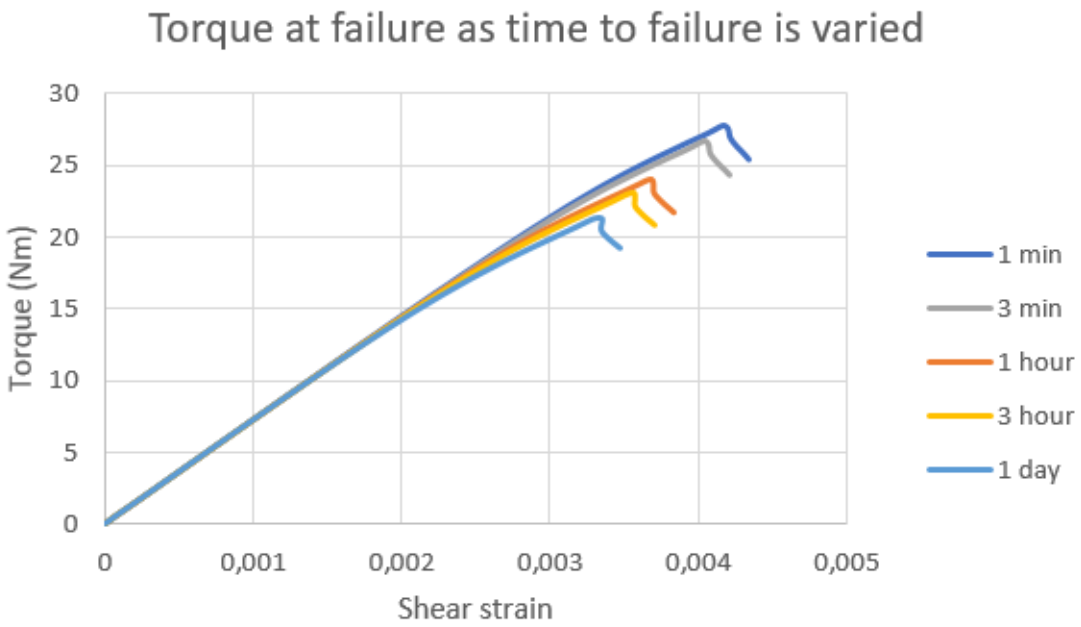

Figure 7.9: Torque as time to failure is varied

As the time to failure increases, the torque at failure decreases.

The soil defined in the Geofuture material model does not have the same strength properties as the soil defined using the Mohr-Coulomb material model. Due to the different properties, one can not compare the results from the two respective numerical simulations. The results from the different Geofuture simulations will only be compared internally. In that way one can determine to which extent strain rates affects the measured strength from the shear vane test.

7.3.2 Further Geofuture Soft Clay 2D Analysis

In order to determine to which extent an increase in time to failure decreases the torque at failure, a 'Torque at Failure-time to failure plot' was created:

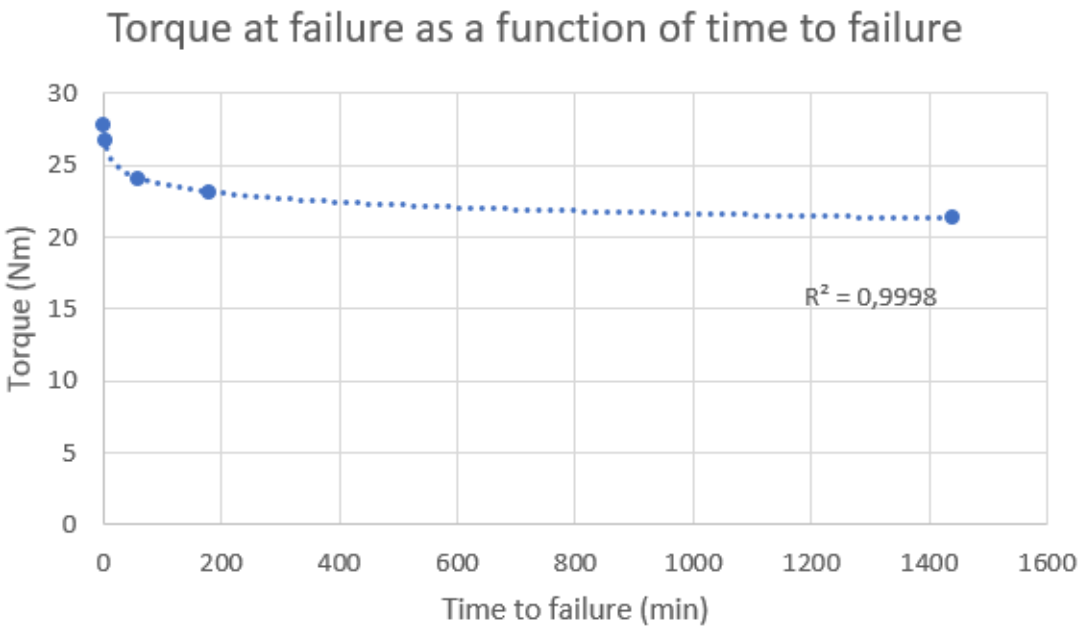

Figure 7.10: Torque at failure as a function of time to failure

When using linear regression a logarithmic correlation between torque at failure and time to failure was observed.

By plotting the logarithm of the time final over time initial (necessary to create a dimensionless value) for each time increase and the relative decrease in torque a linear relationship is achieved.

The relative increase in torque was determined for each load step. In this way, one determines a factor independent of undrained shear strength (the torque at failure is a function of the undrained shear strength of the soil).

The data and the corresponding plot are shown below:

Table 7.2: Percent decrease in torque as a function of a dimensionless time unit

Time to failure	Torque at failure (Nm)	$\text{Log}\left(\frac{t_{final}}{t_{initial}}\right)$	Relative decrease in torque
1 minute	27.76		
		$\text{Log}\left(\frac{3}{1}\right)$=0.477	$\frac{26.74-27.76}{27.76}$= 0.036
3 minutes	26.74		
		$\text{Log}\left(\frac{60}{3}\right)$=1.3	$\frac{24.07-26.74}{26.74}$= 0.099
1 hour (60 minutes)	24.07		
		$\text{Log}\left(\frac{180}{60}\right)$= 0.477	$\frac{23.12-24.07}{24.07}$= 0.039
3 hours (180 minutes)	23.12		
		$\text{Log}\left(\frac{1440}{180}\right)$=0.903	$\frac{21.34-23.12}{23.12}$= 0.07699
1 day (1440 minutes)	21.34		

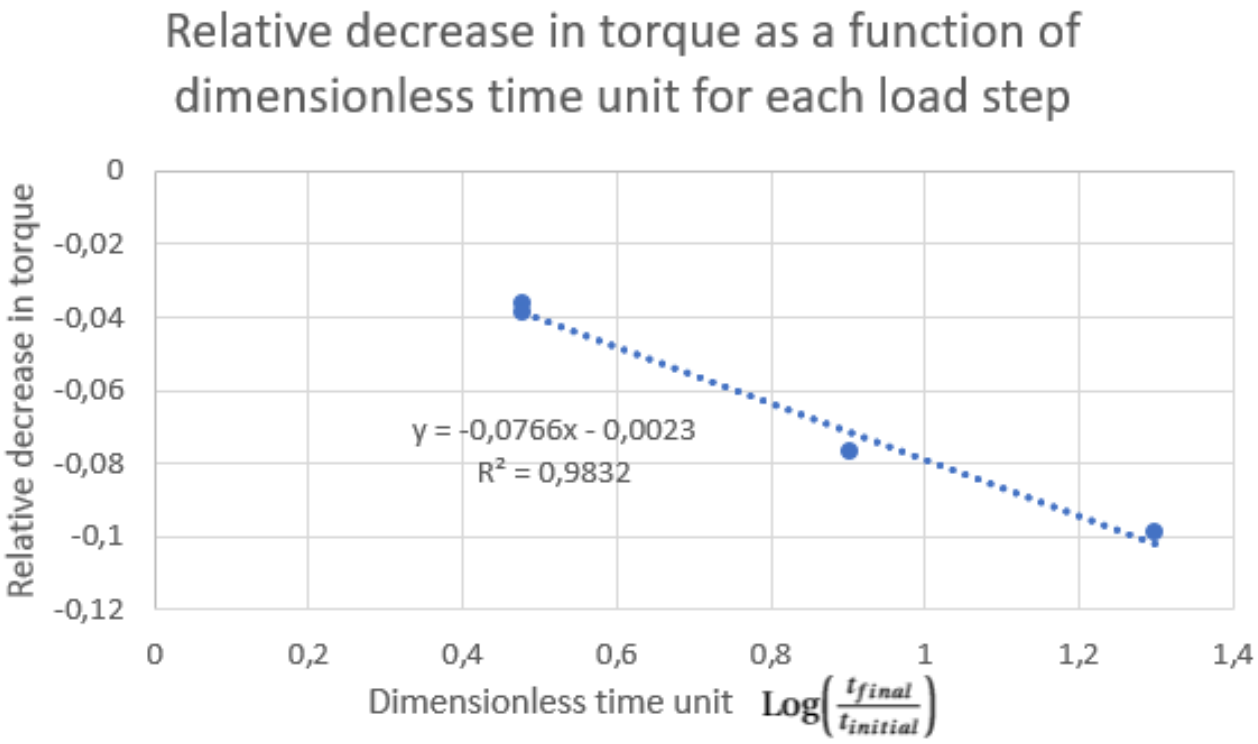

Figure 7.11: Per cent decrease in torque as a function of a dimensionless time unit

From the linear regression, the following linear function describes the relationship between the relative decrease in torque and the increase in time to failure:

$$y = -0.0776x - 0.0023$$

This means a ten fold increase in time to failure, decreases the torque at failure by 7-8 %. Due

to a linear correlation between torque and undrained strength, a ten fold increase in time to failure will also decrease the measured undrained strength by 7-8%.

The results from the numerical simulations fits well with the data observed by Einav and Randolph (2005) from laboratory tests. They observed that a ten fold in time to failure increases the strength by 5-20 %.

When comparing the undrained strength determined from the vane test and the one determined from laboratory tests the time effect can become significant. As the data from the Plaxis analyses show; when time to failure is 3 hours, the torque at failure is 83 % of the torque at failure when time to failure is 1 min. The results seems to indicate that correction factors,μ, have to take time effects into account. Several correlation factors mentioned in Chapter 4 do not incorporate time effects.

Due to the standard time between 1 and 3 minutes when conducting the vane test, the effect of time when comparing two vane test results becomes insignificant. If the time to failure is increased from the lower bound of 1 minute to the upper bound of 3 minutes, then the torque at failure and the measured undrained strength only decreases by 3-4 %.

Due to time effects, one should be aware that the strength from the vane test is non conservative (higher measured shear strength due to a higher strain rate) in comparison to laboratory tests. This is crucial, in situations where the strength in geotechnical design is only based on vane test results.

7.4 Mohr Coloumb Plaxis 3D

7.4.1 Torque at Failure

From the Plaxis simulation, the torque at failure can be determined using the following equation:

$$T_{Plaxis} = 4 \cdot F \cdot M_{stage} \cdot r \cdot H$$

As previously mentioned, a force of 20kN/m was applied to the end of each blade. The vane failed at a M_{stage} value of 0.1004.Thus the torque at failure is:

$$T_{Plaxis} = 4 \cdot 20kN/m \cdot 0.1004 \cdot 0.0275m \cdot 0.11m$$

$$T_{Plaxis} = 24.3Nm$$

The torque at failure from the Plaxis simulation fits well with the result from the hand calculation (24.3 Nm and 23.78 Nm respectively). Percent difference:

$$\left|\frac{24.3Nm - 23.76}{23.76Nm}\right| \cdot 100\% = 2.19\%$$

Just like the Mohr-Coulomb 2D analysis, the similar torques in the Mohr-Coulomb 3D analysis between the Plaxis simulation and the hand calculations seem to indicate the the lack of effect of progressive failure when using the Mohr-Coulomb material model.

In addition, one can observe that the torque at failure is greater in the 3D simulation than in the 2D simulation. This fits well with theory, as the 3D simulations incorporates the contribution from the horizontal surfaces.

A plot of torque as a function of deviatoric strains is shown below. One can observe the post peak softening behavior of the clay.

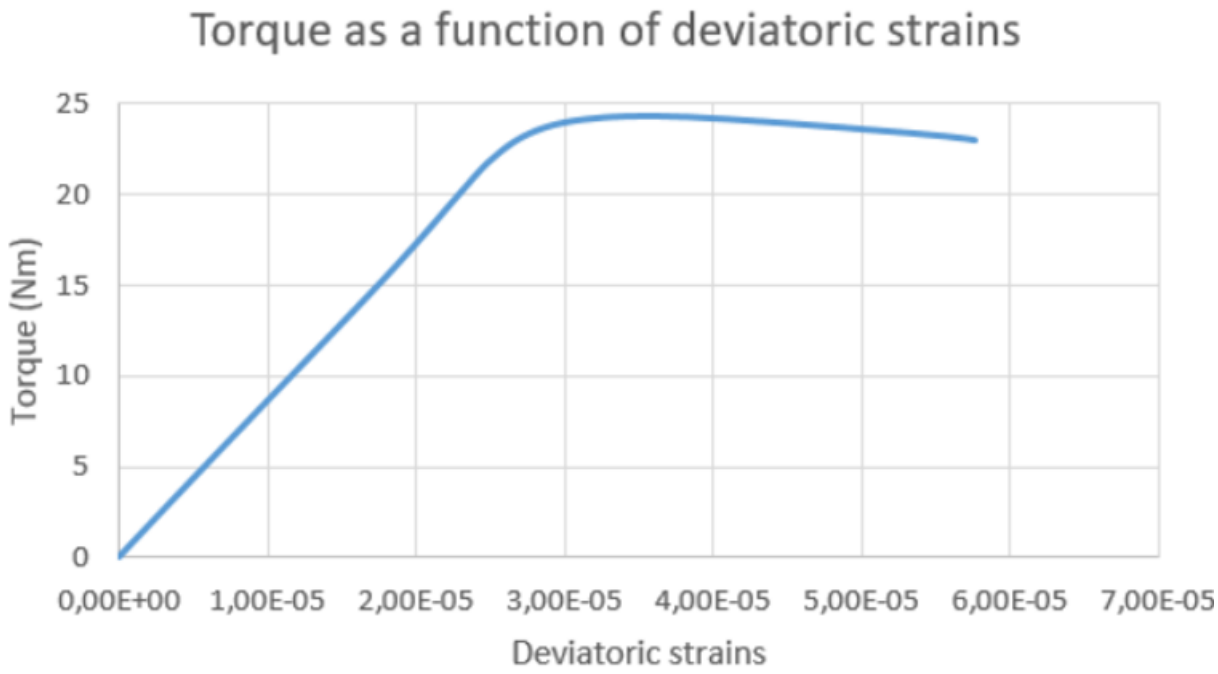

Figure 7.12: Torque as a function of deviatoric stress

7.4.2 Further Analysis

In the following section, figures of three horizontal sections of the vane will be presented. The three horizontal sections are at the top, middle and bottom of the vane. The figures should the circular failure mode during the shear vane test. There are minor differences between the shapes in the top, middle and bottom of the vane, but these are most likely due

to asymmetrical mesh. The mesh at the top, middle and bottom of the vane are not identical. The results fit well with the theoretical circular failure surface.

Total Displacement

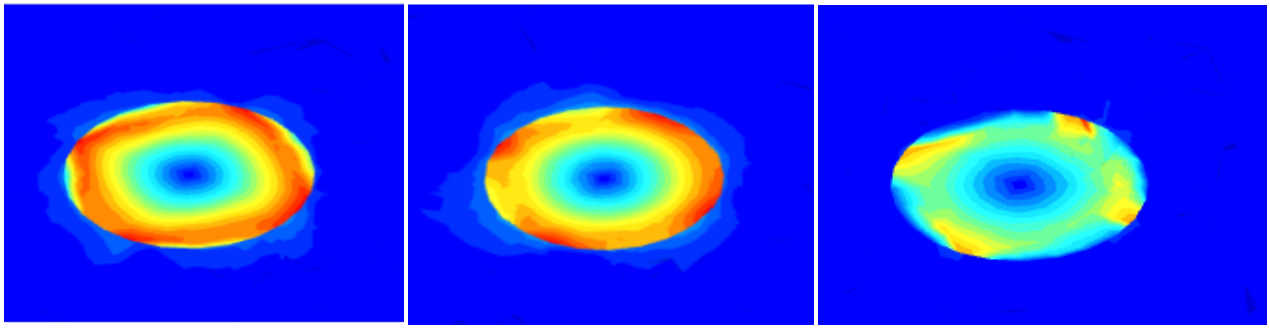

(a) Top of the Vane (b) Middle of the Vane (c) Bottom of the Vane

Incremental Strains

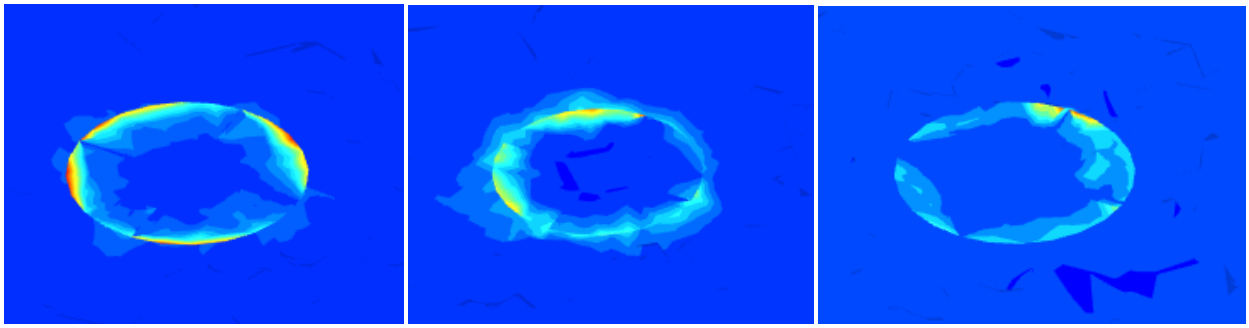

(a) Top of the Vane (b) Middle of the Vane (c) Bottom of the Vane

Total strains

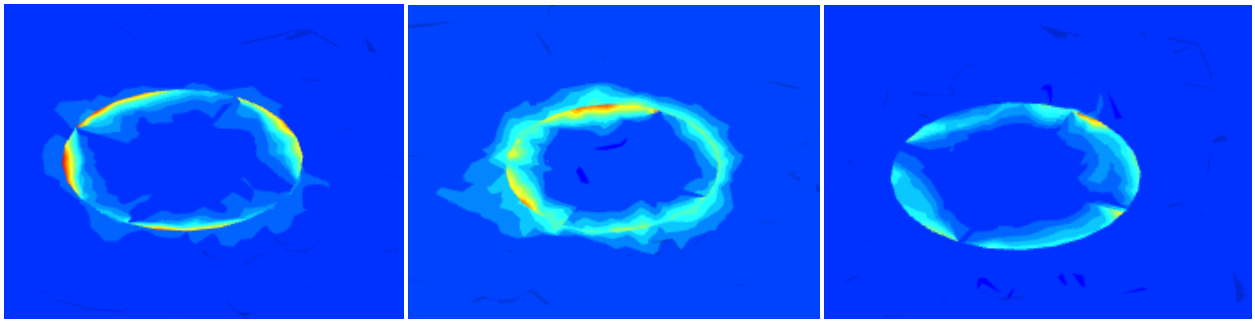

(a) Top of the Vane (b) Middle of the Vane (c) Bottom of the Vane

7.5 NGI ADP-Plaxis 3D

7.5.1 Torque at Failure

For each simulation the torque was determined by the same formula previously used:

$$T = 4 \cdot F \cdot M_{stage} \cdot R \cdot H$$

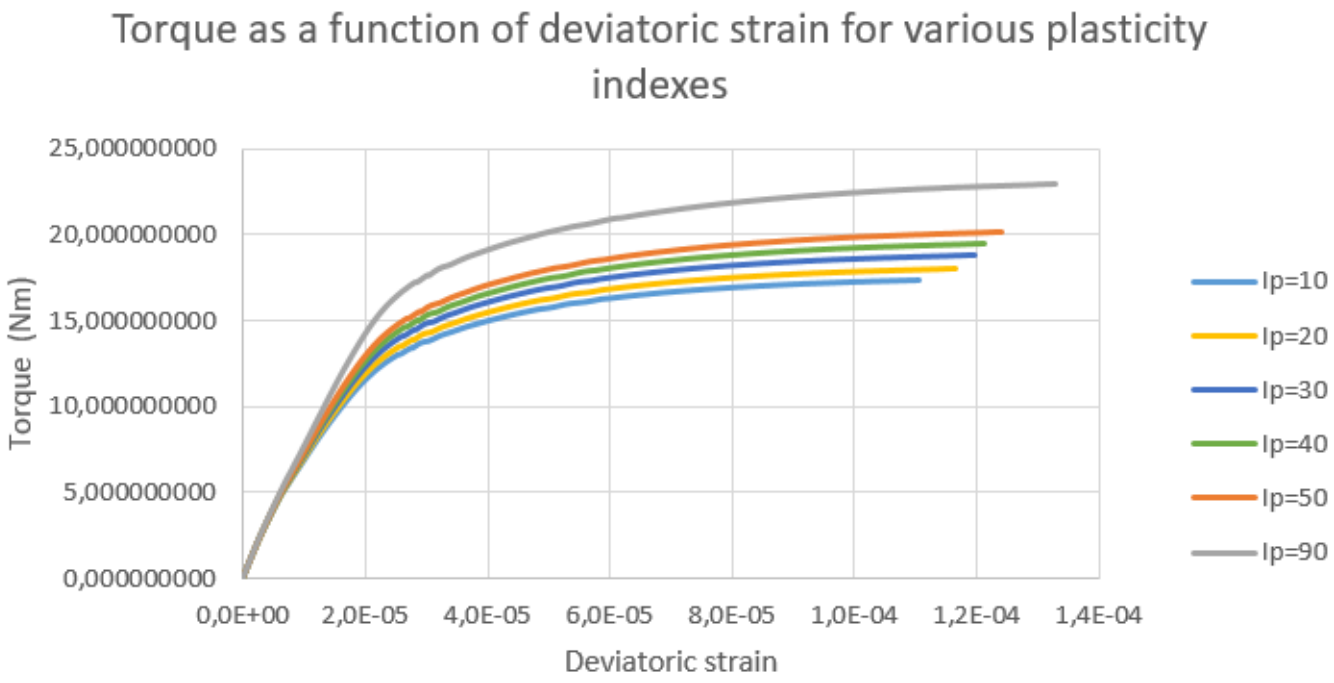

Figure 7.16: Torque as a function of deviatoric strain for various plasticity indexes

As one can observe, an increase in plasticity index (decrease in anisotropy) increases the torque at failure. The NGI ADP model does not factor in softening behavior of clays (Undrained B analysis).

The soil defined using the NGI ADP material model does not have the same strength properties as the soil defined using the Mohr-Coulomb and Geofuture material model. Thus, the torque at failure determined from each material model can not be compared with each other. The results from the NGI ADP simulations will only be compared internally in order to determine to which extent anisotropy affects the measured strength from the shear vane test.

7.5.2 Further NGI ADP Analysis

As one can observe from Figure 7.16, a decrease in anisotropy (increase in plasticity index), increases the torque at failure. In order to determine to which extent a decrease in anisotropy increases the torque at failure further analysis is necessary.

A ”peak torque-plasticity index” plot was created:

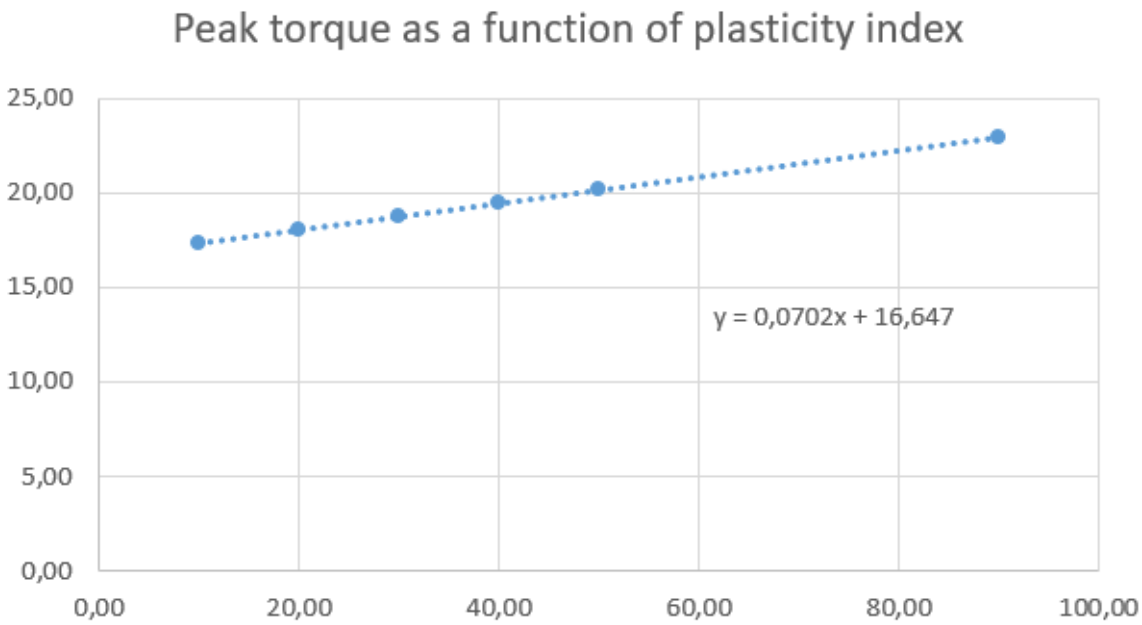

Figure 7.17: Peak torque as a function of plasticity index

One can observe a linear correlation between torque at failure and plasticity index.

Using the same methodology as in subsection 7.3.2, one can determine a correlation that is independent of the strength of the soil (All the torques in the plot above are a function of the input parameter s_u^A in Plaxis).

The data and the corresponding analysis are shown in Table 7.3 below:

Table 7.3: Correlation between increase in plasticity and increase in torque

I_p	Torque at failure (Nm)	Increase in I_p	Relative increase in torque	$\frac{\text{Relative increase in torque}}{\text{increase in } I_p}$
10 %	17.32			
		20 % -10% = 10%	$\frac{18.07-17.32}{17.32} = 0.043$	$\frac{0.0403}{10} = 0.0043$
20 %	18.07			
		20 % -10% = 10%	$\frac{18.76-18.07}{18.07} = 0.038$	$\frac{0.038}{10} = 0.0038$
30 %	18.76			
		20 % -10% = 10%	$\frac{19.46-18.76}{18.76} = 0.037$	$\frac{0.037}{10} = 0.0037$
40 %	19.46			
		20 % -10% = 10%	$\frac{20.15-19.46}{19.46} = 0.035$	$\frac{0.035}{10} = 0.0035$
50 %	20.15			
		90 % -50% = 40%	$\frac{22.96-20.15}{20.15} = 0.139$	$\frac{0.139}{40} = 0.0035$
90 %	22.96			

From the fifth column one can observe a more or less constant relative increase in torque per increase in I_p for each load step. The average for all 5 load steps is 0.376 % increase in torque per % increase in plasticity.

$$\frac{0.0043 + 0.0038 + 0.0037 + 0.0035 + 0.0035}{5} = 0.00376$$

Due to a linear correlation between torque and undrained shear strength, the undrained shear strength also increases by 0.376 % per % increase in plasticity. Alternatively, an increase in plasticity of 10 %, increases the torque by 3.76 % . For example, when comparing a highly plastic clay (I_p of 40 %) and a low plastic clay (I_p of 7 %), the torque at failure of the highly plastic clay will be 12.4 % higher than the low plastic clay due to soil anisotropy.

7.5.3 Comparing the Plaxis Results with known Correction Factors

In this subsection the results from the NGI ADP analyses will be compared with the Scandinavian correction factors. The correction factors are described in detail in Chapter 4.

The correction factors are shown in the figure below:

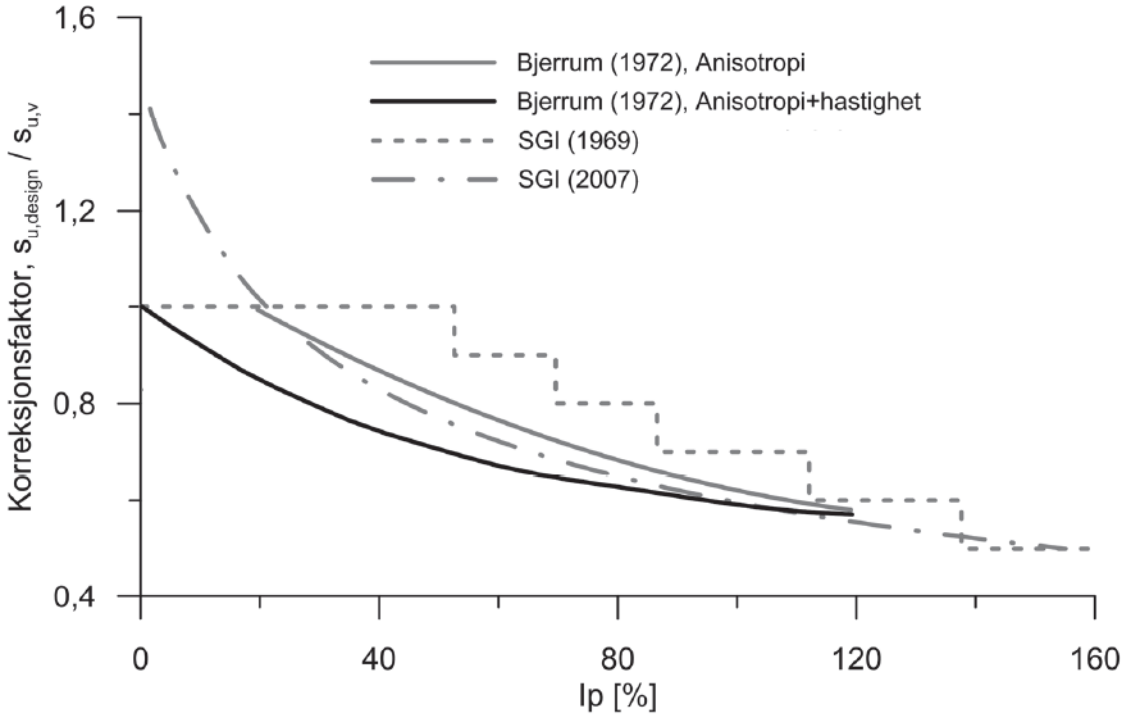

Figure 7.18: Overview of the different correction factors (after (NTNU, 2014)

The same methodology will be used for every correction factor when comparing the different correction factors with the Plaxis results.

As previously mentioned, the correction factors are meant to ”correct” the strength determined from the shear vane test. The methodology behind the comparisons is; Regardless of the plasticity index of the soil, the design strength ($s_{u,design}$) which is based on the shear vane test should be the same after implementing the correction factor.

$$s_{u,design} = \mu \cdot s_{u,vane}$$

For the comparisons done in this report, clays with plasticity index 20% and 40% were chosen. A clay with plasticity of 20 % was chosen , as a plasticity index less than 20% is outside the domain of the original Bjerrum correction factor.

The design strength ($s_{u,design}$) should be independent of the plasticity of the soil :

$$s_{u,design} = s_{u,design}$$

$$s_{u,(design)_{I_{p=20\%}}} = s_{u,(design)_{I_{p=40\%}}}$$

$$\mu_{(I_{p=20\%})} \cdot s_{u,(vane)_{I_{p=20\%}}} = \mu_{(I_{p=40\%})} \cdot s_{u,(vane)_{I_{p=40\%}}}$$

Rearranging the equation:

$$\frac{s_{u,(vane)_{I_{p=40\%}}}}{s_{u,(vane)_{I_{p=20\%}}}} = \frac{\mu_{(I_{p=20\%})}}{\mu_{(I_{p=40\%})}}$$

The NGI ADP Plaxis analysis showed a 0.376 % increase in shear strength per % increase in plasticity. Thus the clay with plasticity index of 40% will have a shear strength 7.52 % greater than the clay with plasticity index of 20 %.

$$\frac{0.376\% \text{ increase in strength}}{\% \text{ increase in plasticity}} \cdot (40-20)\% \text{ increase in plasticity} = 7.52\%$$

$$\frac{s_{u,(vane)_{I_{p=40\%}}}}{s_{u,(vane)_{I_{p=20\%}}}} = 1.0752$$

Comparison with Bjerrum's Original Correction Factor

In 1972 Bjerrum proposed a correction factor based solely on anisotropy.
From Figure 7.19 below, the correction factor of each plasticity index (I_p= 20 % and I_p= 40 %) can be determined:

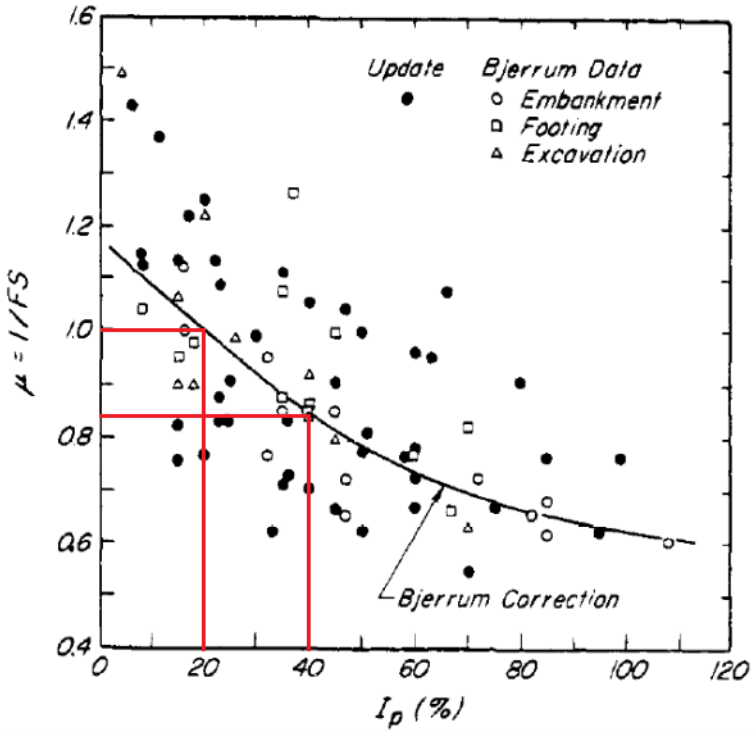

Figure 7.19: Bjerrum's original correction factor (after (Terzaghi et al., 1996))

From the figure:

$$\mu_{(I_{p=20\%})} \approx 1.0$$

$$\mu_{(I_{p=40\%})} \approx 0.85$$

Thus

$$\frac{\mu_{(I_{p=20\%})}}{\mu_{(I_{p=40\%})}} = \frac{1.0}{0.85} = 1.176$$

.

$$\frac{\mu_{(I_{p=20\%})}}{\mu_{(I_{p=40\%})}} = 1.176 \neq 1.0752 = \frac{s_{u,(vane)_{I_{p=40\%}}}}{s_{u,(vane)_{I_{p=20\%}}}}$$

The equation above shows that the Plaxis analysis does not yield the same result as the original Bjerrum correction factor.

However as one can observe from figure 7.19 above, there is a significant scatter in the data points. The correction factor, which is an average of all the points, is therefore only a rough estimate. In addition, the original Bjerrum correction factor is based solely on soil anisotropy. The effect of strain rate might explain the discrepancy. The Geofuture 2D analysis seemed to suggest that strain rates affect the results from the shear vane test.

Comparison with Bjerrum's second correction factor

In 1972 Bjerrum proposed a second correction factor. Contrary to the original correction factor, the second correction factor also takes strain rate effects into account in addition to soil anisotropy.

From Figure 7.20, the correction factor of each plasticity index (I_p= 20 % and I_p= 40 %) can be determined.

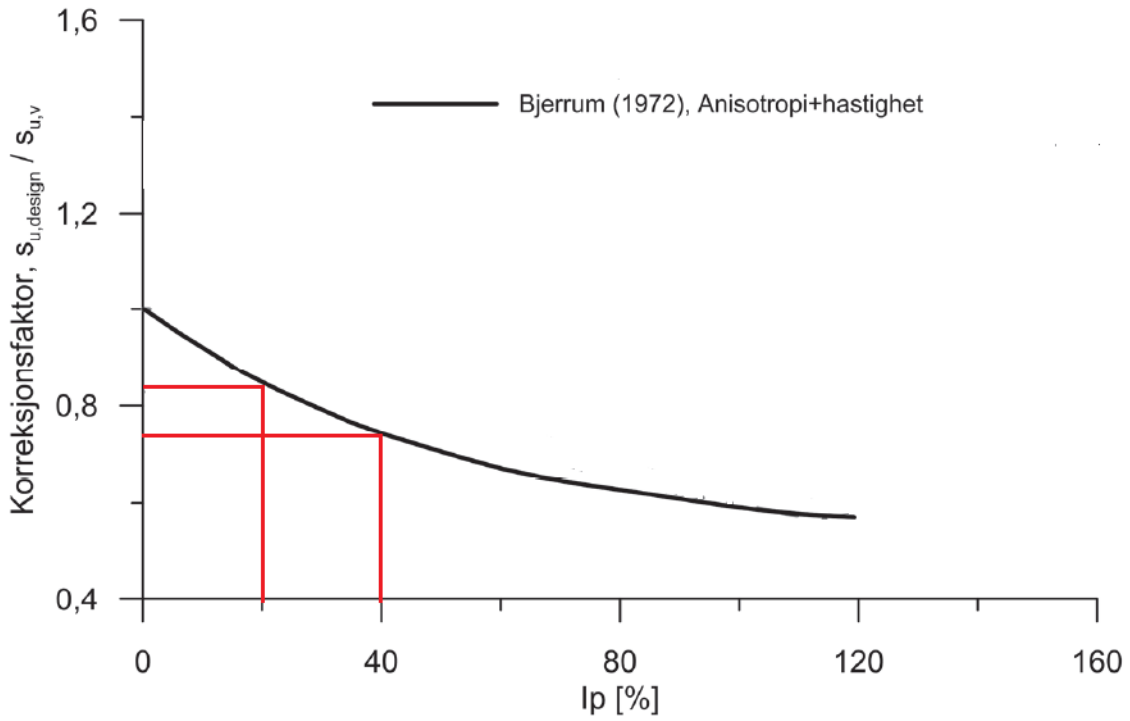

Figure 7.20: Bjerrum's second correction factor (modified after (NTNU, 2014))

From the figure:

$$\mu_{(I_{p=20\%})} \approx 0.83$$

$$\mu_{(I_{p=40\%})} \approx 0.76$$

Thus

$$\frac{\mu_{(I_{p=20\%})}}{\mu_{(I_{p=40\%})}} = \frac{1.0}{0.85} = 1.09$$

.

$$\frac{\mu_{(I_{p=20\%})}}{\mu_{(I_{p=40\%})}} = 1.09 \approx 1.0752 = \frac{s_{u,(vane)_{I_{p=40\%}}}}{s_{u,(vane)_{I_{p=20\%}}}}$$

The Plaxis analysis yields approximately the same result as the second correction factor.

The similar results when using the the second Bjerrum correction factor suggests that strain rate effects should be incorporated in the correction factor.
This fits well with the findings from the Geofuture 2D analysis ; strain rate effects should be taken into account when determining the strength of the soil using the shear vane test.

Comparison with the Swedish Correction Factors

SGI has proposed two correction factors; the original from 1969 and the updated one from 2007. As one can observe in figure 7.21 below, the original correction factor has a constant value at plasticity indexes of 20% and 40 %. Thus one can immediately see that this correction factor does not fit the Plaxis results. The original correction factor will not be discussed in further detail. Comparison between the Plaxis results and the updated correction factor:

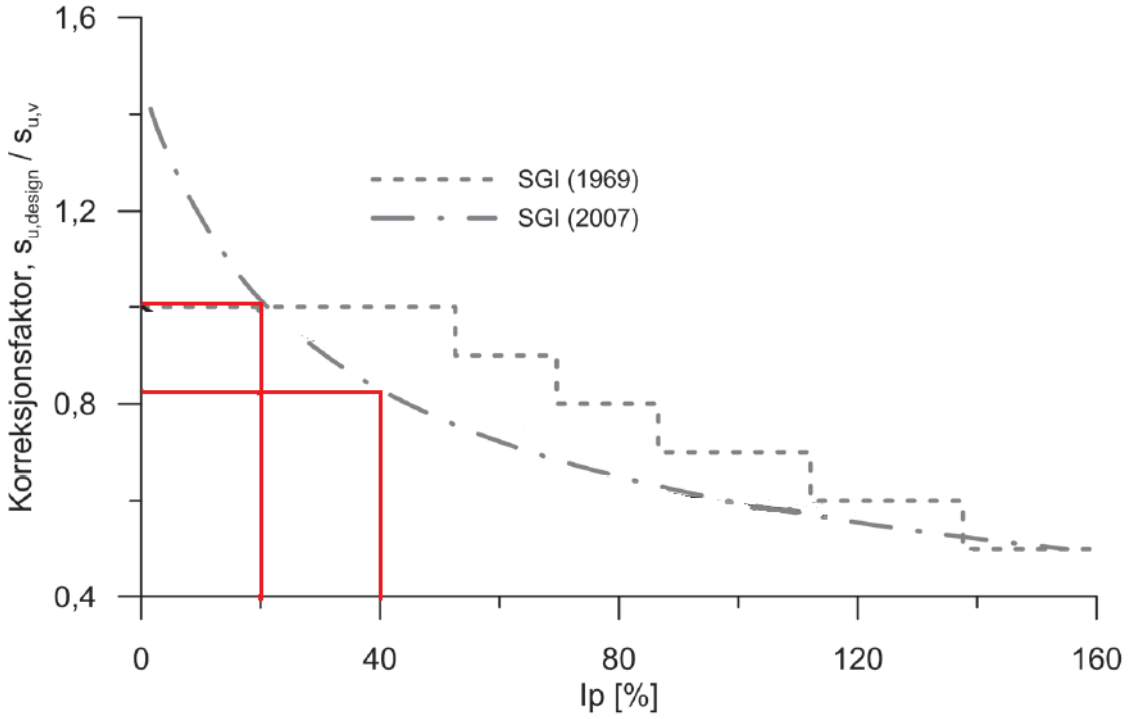

Figure 7.21: Swedish correction factors (modified after (NTNU, 2014))

From the figure:

$$\mu_{(I_{p=20\%})} \approx 1.01$$

$$\mu_{(I_{p=40\%})} \approx 0.82$$

Thus

$$\frac{\mu_{(I_{p=20\%})}}{\mu_{(I_{p=40\%})}} = \frac{1.01}{0.82} = 1.24$$

.

$$\frac{\mu_{(I_{p=20\%})}}{\mu_{(I_{p=40\%})}} = 1.24 \neq 1.0752 = \frac{s_{u,(vane)_{I_{p=40\%}}}}{s_{u,(vane)_{I_{p=20\%}}}}$$

Out of all the correction factors, the updated Swedish correction factor is the less representative of the Scandinavian correction factors.

Conclusion

Based on the results from the Plaxis analysis, the second Bjerrum correction factor (which takes soil anisotropy and time effects into account) seems to be the best fit. It is reasonable that the correction factor that incorporates time effects (in addition to soil anisotropy) is the best fit, as the Geofuture 2D analysis seemed to indicate that time effects affect results in the shear vane test.

Although, the second Bjerrum correction factor seems is the function with the best fit, there is a considerable uncertainty in the analysis. One can not say for certain that is it the best fit. Further analysis (bigger sample size) is necessary. However the analysis conducted gives us an indication of which correction factor is the best fit. There are a couple of reasons why there is considerable uncertainty in the analysis.

First of all, the correction factors are an average of data has a lot of scatter and thus have a significant uncertainty.

In addition there is uncertainty in the plasticity indexes of the soils tested in Plaxis. Plaxis does not have plasticity index as an input parameter ($\frac{s_u^{DSS}}{s_u^A}$ is an input parameter in Plaxis). The plasticity of the soil tested were determined the following empirical relation developed by (Thakur, 2013):

$$\frac{s_u^{DSS}}{s_u^A} = 0.63 + 0.00425 \cdot (I_p - 10)$$

The empirical relation is based on a approximated trend line from tests on Norwegian Clay.

Chapter 8

Conclusion

8.1 Summary and Conclusion

The objective of this report has been to investigate to which extent progressive failure (softening), rate effects and anisotropy affects the measured shear strength from the shear vane test. Each effect has been investigated individually.

When determining the effect of progressive failure, the Mohr-Coulomb material model was applied. In order to simulate a softening material, the dilatency angle was set to -1 °. The effect of progressive failure was analyzed by comparing the results from the numerical simulations and hand calculations.

The Geofuture material model was applied, when determining the effects of strain rate during the shear vane test. The effects of strain rate were analyzed by varying the time to failure for each simulation. The Geofuture material model also incorporates softening and anisotropy effects. However the Geofuture simulations were conducted exclusively to investigate strain rate effects. The degree of anisotropy and softening were kept constant for each simulation.

When determining to which extent anisotropy affects the measured strength from the shear vane test, the NGI ADP material model was applied. The degree of anisotropy was measured by the plasticity index of the soil. For each simulation, the active strength stayed constant while the direct and passives strengths varied as a function of plasticity index.

8.1.1 Effect of Softening

The numerical simulations conducted using the Mohr-Coulomb material model yielded approximately the same torque at failure as the hand calculation. The percent difference between the 2D analysis and the hand calculation was 3.8 %. The percent difference per cent difference between the 3D analysis and the hand calculation was 2.2 %. The numerical simulations seem to indicate that the effect of progressive failure can be neglected when using the Mohr-Coulomb material model. This fits well with the finding from (Cadling and Odenstad, 1948). Cadling and Odenstad (1948) argued that the effect of progressive failure can be neglected in the shear vane test.

8.1.2 Effect of Strain Rate

From the numerical simulations conducted using the Geofuture material model, it was found that a ten fold increase in "time to failure" decreases the measured torque and shear strength by 7-8 %. The findings from the numerical simulations fits well with the findings from Einav and Randolph (2005). Based on data from laboratory tests Einav and Randolph (2005) observed that a ten fold in time to failure increases the strength by 5-20 %.

The time to failure difference between laboratory test and the shear vane test, can be quite significant. A standard time to failure during the shear vane test has been set to 1-3 minutes. Meanwhile laboratory tests often go to failure after a couple of hours. Due to the different strain rates, there will be a discrepancy between laboratory tests and shear vane tests.

The numerical analysis using the Geofuture material model seem to indicate that strain rate will play a role in the measured shear strength from the shear vane test. Thus, the numerical simulations seem to suggest that correction factors should take strain rate effects into account.

8.1.3 Effect of Anisotropy

Based on the numerical simulations run using the NGI ADP material model, the shear strength measured from the shear vane test increases by 3-4 % per 10% increase in plasticity index.

The results from the numerical simulations using the NGI ADP material model suggests that anisotropy should be taken into account in the correction factors.

8.2 Further Work

For further work one should conduct more numerical simulations in order to examine how the resistance and the failure mechanism of the soil is effected as the effects of progressive failure, strain rate and anisotropy happen simultaneously.

This can be investigated by using the Geofuture material model. As previously mentioned, the material model incorporates rate effects, softening and anisotropy. In this report the effects of progressive failure, strain rate and anisotropy have been investigated individually.

For further work one should investigate the effect of anisotropy and progressive failure using the Geofuture material model.

The results from the Mohr-Coulomb analysis seem to indicate that effect of progressive failure can be neglected when using the Mohr-Coulomb material model. The Geofuture material model incorporates softening differently than the Mohr-Coulomb material model. As a result the effect of progressive failure could be more significant when using the Geofuture model. This should be further investigated.

Based on the Mohr-Coulomb 2D simulation, the shear vane test simulates a direct simple shear test for a horizontal section. This could be further analyzed using the Geofuture model.

In addition, one could compare the shear stress at failure on the vertical and horizontal planes in order to determine the degree of anisotropy during the shear vane test when using the Geofuture material model.

Furthermore, by conducting more simulations one can estimate with less uncertainty which of the correction factors is the most representative for Norwegian clays. Based on the results from this report, the correction factor should incorporate both strain rate effects and anisotropy. The results seemed to indicate that the Bjerrum's second correction factor is the most representative. This should be verified with further simulations.

Bibliography

Aas, G. (1965). A study of the effect of vane shape and rate of strain on the measured values of in-situ shear strength of clays.

Aas, G. (1979). Vurdering av korttidsstabilitet i leire på basis av udrenert skjaerfasthet.NGM -79 helsingfors.

Aas, G., Lacasse, L., Lunne, T., and Høeg, K. (1986). Use of in situ tests for foundation design in clay.asce proc. in-situ '86, virginia, usa, pp 589-600.

Andersen, K. and Lunne, T. (2007). Bearing capacity under cyclic loading — offshore, along the coast, and on land.

Biscotin, G. and Pestana, J. (2001). Influence of peripherical velocity on vane shear strength of an artificial clay.

Bjerrum, L. (1972). Embankments on soft ground.

Cadling, L. and Odenstad, S. (1948). The vane borer, royal swedish geotechnical institute, proceedings no. 2, stockholm, pp 88.

Chandler, R. (1988). The in-situ measurement of the undrained shear strength of clays using the field vane.in vane shear strength testing in soils:field and laboratory studies.

Einav, I. and Randolph, M. (2005). "combining upper bound and strain path methods for evaluating penetration resistance"int.j.numer.methods eng.,63(14),1991-2016.

Fauskerud, O. A., Gylland, A. S., Athanasiu, C., Christensen, S. O., Havnegjerde, C. R., Tørum, E., and Gylland, A. S. (2013). Bruk av anisotropiforhold i stabilitetsberegninger i sprøbrud-dmaterialer.

Graham, J., Crooks, J., and Bell, A. (1983). Time effects on the stress strain behaviour of natural soft clays.

Gylland, A. (2012). "material and slope failure of sensitive clays".doctora theses ntny,2012:352.

Gylland, A., Jonstad, H., and Nordal, S. (2012). Failure geometry around a shear vane in sensitive clay.

Jamiolkowski, M., Ladd, C. C., Germaine, J., and Lancellotta, R. (1985). "new developments in field and laboratory testing of soils", proceedings of the 11th international conference on soil mechanics and foundation engineering.

Jonnson, M. and Sellin, C. (2012). Correction of shear strength in cohesive soil.

Karlsrud, K., Lunne, T., Kort, D., and Strandvik, S. (2005). CPTU correlations for clays. in proc. of 16th icsmge, osaka. mill press, rotterdam: 693 -702.

Ladd, C. (1991). "stability evaluation during staged construction."jnl. of the geo.eng. div., ASCE.117,gt4:540-615.

Ladd, C. and Foott, R. (1974). New design procedure for stability of soft clays.

Larsson, R., Sällfors, G., Bengtsson, P.-E., Alen, C., Bergdahl, U., and Eriksson, L. (2007). Skjuvhållfasthet-utvärding i kohesionsjord.

NTNU (2014). Tolkning av aktiv udrenert skjærfasthet fra vingebor,ntnu rapport levert av NIFS.

Plaxis (2016). Material models manual.

Rønningen, J. (2017). Geofuture soft clay model, user manual.

Sheahan, T., Lad, C., and Germaine, J. (1996). Rate-dependent undrained shear behavior of saturated clay, journal of geotechnical engineering, asce, 2, pp. 99-108.

Terzaghi, K., Peck, P., and Mesri, G. (1996). Soil mechanics in engineering practice. 3rd edition.

Thakur, V. (2013). NIFS naturfare, en nasjonal satsning på sikkerhet i kvikkleireområder.